

**Identifizierung molekulargenetischer Ursachen von
seltenen angeborenen Immundefekten am Beispiel der
Hyper-IgE Syndrome**

Benedikt D. Spielberger



München 2021

Aus der Kinderklinik und Kinderpoliklinik
im Dr. von Haunerschen Kinderspital
der Ludwig-Maximilians-Universität München

**Identifizierung molekulargenetischer Ursachen von seltenen angeborenen Immundefekten
am Beispiel der Hyper-IgE Syndrome**

Dissertation
zum Erwerb des Doktorgrades der Medizin
an der Medizinischen Fakultät
der Ludwig-Maximilians-Universität zu München

vorgelegt von
Benedikt Daniel Spielberger
aus
München
im Jahr
2021

Mit Genehmigung der Medizinischen Fakultät
der Universität München

Berichterstatter: Prof. Dr. med. Ellen D. Renner

Mitberichterstatter: Prof. Dr. K. Spiekermann
Prof. Dr. H. Schulze-Koops
PD Dr. Dr. E. Strobel

Mitbetreuung durch die
promovierte Mitarbeiterin: Dr. Beate Hagl

Dekan: Prof. Dr. med. dent. Reinhard Hickel

Tag der mündlichen Prüfung: 18.02.2021

Einleitende Zusammenfassung
der schriftlichen kumulativen Promotion

gemäß §4a der Promotionsordnung für die Fakultät

der Ludwigs-Maximilians-Universität München

vom 1. Juni 1983

in der konsolidierten Fassung der elften Änderungssatzung vom 15. September 2016

Eidesstattliche Versicherung

Benedikt Daniel Spielberger

Ich erkläre hiermit an Eides statt, dass ich die vorliegende Dissertation mit dem Thema **Identifizierung molekulargenetischer Ursachen von seltenen angeborenen Immundefekten am Beispiel der Hyper-IgE Syndrome**

selbstständig verfasst, mich außer der angegebenen keiner weiteren Hilfsmittel bedient und alle Erkenntnisse, die aus dem Schrifttum ganz oder annähernd übernommen sind, als solche kenntlich gemacht und nach ihrer Herkunft unter Bezeichnung der Fundstelle einzeln nachgewiesen habe.

Ich erkläre des Weiteren, dass die hier vorgelegte Dissertation nicht in gleicher oder in ähnlicher Form bei einer anderen Stelle zur Erlangung eines akademischen Grades eingereicht wurde.

Freiburg, 10.03.2021

Benedikt Spielberger

Unterschrift Doktorand

Inhaltsverzeichnis

1	Abkürzungsverzeichnis	7
2	Beitrag zu den Publikationen	8
2.1	Beitrag zur Publikation „Challenges of genetic counseling in patients with autosomal dominant diseases, such as the Hyper-IgE syndrome (STAT3-HIES)“	8
2.2	Beitrag zur Publikation „Somatic alterations compromised molecular diagnosis of DOCK8 hyper-IgE syndrome caused by a novel intronic splice site mutation“	9
3	Einleitung	12
4	Zusammenfassung	18
5	Summary	20
6	Schriftenverzeichnis	22
6.1	Originalarbeit: Challenges of genetic counseling in patients with autosomal dominant diseases, such as the hyper-IgE syndrome (STAT3-HIES)	22
6.2	Originalarbeit: Somatic alterations compromised molecular diagnosis of DOCK8 hyper-IgE syndrome caused by a novel intronic splice site mutation	26
7	Literaturverzeichnis	49
8	Danksagung	51
9	Publikationsliste	53

1 Abkürzungsverzeichnis

AD-HIES	Autosomal-dominantes Hyper-IgE Syndrom
AR-HIES	Autosomal-rezessives Hyper-IgE Syndrom
DNA	Desoxyribonukleinsäure
DOCK8	Dedicator of cytokinesis 8
ESID	European society for immunodeficiencies
GEF	G-protein exchange factor
HHV3	Humanes Herpesvirus 3
HIES	Hyper-IgE Syndrom
HSV1/2	Herpes simplex-Virus 1/2
HSZT	Hämatopoetische Stammzelltransplantation
IL6	Interleukin 6
IL10	Interleukin 10
NGS	Next Generation Sequencing
NK-Zellen	natürliche Killerzellen
PBMC	periphere mononukleäre Zellen
PID	Primärer Immundefekt
STAT1	Signal transducer and activator of transcription 1
STAT3	Signal transducer and activator of transcription 3
STAT5	Signal transducer and activator of transcription 5
Tem	effector memory T-Zellen
Temra	exhausted effector memory T-Zellen
Tyk2	Tyrosinkinase 2
WES	Whole-exome sequencing
WGS	Whole-genome sequencing

2 Beitrag zu den Publikationen

Nach methodischer Einarbeitung in die Durchführung von Polymerase Kettenreaktion (PCR) und deren Sequenzierung, sowie Planung, Durchführung und Analyse von intrazellulären Färbungen mittels Durchflusszytometrie (FACS) begann ich mit der Bearbeitung eines eigenständigen Projekts.

2.1 Beitrag zur Publikation „ Challenges of genetic counseling in patients with autosomal dominant diseases, such as the Hyper-IgE syndrome (STAT3-HIES)“

Zur Publikation „Challenges of genetic counseling in patients with autosomal dominant diseases, such as the hyper-IgE syndrome (STAT3-HIES)“ erstellte ich gemeinsam mit Frau Prof. Ellen Renner und Frau Dr. Beate Hagl das Studienprotokoll und –design. In dieser Publikation deckte ich die Ursache für eine überproportionale Häufung an STAT3-HIES bei den Nachkommen gesunder Eltern auf. Mein Beitrag bestand darin, die Hypothese einer Keimbahnmutation im Spermia des Vaters zu untersuchen. Hierfür warb ich bei den betroffenen Familien um Zustimmung an der wissenschaftlichen Studie teilzunehmen. Ich etablierte die Sequenzierung von *STAT3* aus Spermien in Kooperation mit Frau Prof. Katja Anslinger und Frau Birgit Bayer aus dem Institut für Rechtsmedizin der LMU München. Ich führte selbstständig die genetische Untersuchung von *STAT3* aus Spermien im Labor von Frau Prof. Ellen Renner durch. Des Weiteren bestand mein Beitrag in der Erhebung und Analyse der klinischen Daten, weiterer laborchemischer Parameter, Erstellung von HIES-Scores und der Interpretation der Ergebnisse sowie der Korrespondenz mit Koautoren zur Gewinnung der Daten und des Untersuchungsmaterials. Dr. Kathrin Siepermann, Dr. Gregor Dückers und Prof. Tim Niehues betreuten Patienten. Dr. Christina Wöllner führte die Mutationsanalyse bei einem Patienten durch und Prof. Bodo Grimbacher diagnostizierte und betreute Patienten, die in der Publikation enthalten sind. Julie Sawalle-Belohradsky führte die *STAT3* PCR aus

genomischer DNA der betroffenen Kinder durch. Prof. Bernd Belohradsky betreute Patienten der Publikation vor der Übergabe an Prof. Ellen Renner. Gemeinsam mit Frau Prof. Ellen Renner schrieb ich hauptverantwortlich unter Beteiligung aller Autoren das Manuskript und brachte es zur erfolgreichen Publikation im *Journal of Allergy and Clinical Immunology*. Alle Autoren beteiligten an der Manuskripterstellung und gaben ihr Einverständnis zur Veröffentlichung der finalen Manuskriptversion.

2015 konnte ich die Ergebnisse dieses Forschungsprojektes im Rahmen der Summer School der European Society for Immunodeficiencies (ESID) vorstellen.

2.2 Beitrag zur Publikation „Somatic alterations compromised molecular diagnosis of DOCK8 hyper-IgE syndrome caused by a novel intronic splice site mutation“

Für die Publikation „Somatic alterations compromised molecular diagnosis of DOCK8 hyper-IgE syndrome caused by a novel intronic splice site mutation“ erarbeitete ich zusammen mit Frau Prof. Ellen Renner und Frau Dr. Beate Hagl das Studienprotokoll und –design, und unterstützte Frau Prof. Ellen Renner erfolgreich beim Einwerben von Forschungsgeldern der Wilhelm Sander-Stiftung. Für diese Publikation erhob und analysierte ich zunächst klinische Daten einer Patientenfamilie mit zwei Kindern mit dem klinischen Bild eines HIES und unklarer krankheitsverursachender Mutation. Im Rahmen der experimentellen Arbeit führte ich genetische und immunologische Untersuchungen der Patienten, ihren Familienmitgliedern und von gesunden Kontrollpersonen durch. Hierfür etablierte ich Verfahrensprotokolle für Durchflusszytometrische Untersuchungen wie die Stimulation und Analyse der Phosphorylierung von STAT1 (pSTAT1) und STAT5 (pSTAT5) in PBMCs und expandierten T-Zellen (nicht in der finalen Publikation enthalten) und von STAT3 (pSTAT3) in Fibroblasten

sowie die intrazelluläre Färbung für DOCK8 mit insgesamt acht Oberflächenmarkern (Fig. 4 und 5). Darüber hinaus etablierte ich das Einzelzell-Sorting für die anschließende Sequenzierung von *DOCK8* DNA und RNA in verschiedenen Zellsubpopulationen (Fig. 4 und 5). Zusätzlich etablierte ich die in der Publikation im Text erwähnte Luminex-basierten Analysen sowie das Serum-Inkubations-Assay (Supplementary Fig. S1), um Auto-Antikörper als mögliche Ursache der fehlenden Stimulierbarkeit von pSTAT3 auf Interleukin-6 auszuschließen. Die Etablierung der Auto-Antikörper Untersuchung wurde von Dr. Anne Puel durch ihre Vorerfahrungen bei der Etablierung einer ähnlichen Methode unterstützt. Hierbei gelang es mir IL6, IL6R und gp130 an fluoreszierende beads zu koppeln und mittels Luminex-Assay die Bindung von Proteinen aus Patientenserum darzustellen. Zusammen mit Prof. Jordan Orange und Prof. Ellen Renner analysierte ich die Daten des whole-exome Sequencing. Gemeinsam mit Shira Verduin, Dr. Isaac Njman, Dr. Beate Hagl und Prof. Mirjam von Gjin analysierte ich die Daten des whole-genome sequencing. Hierbei zeigte sich ARHGAP32 als vielversprechendes Kandidatengen, sodass ich hierfür Transfektionsexperimente mit Patientenzellen etablierte und erfolgreich durchführte (Supplementary Fig. S2). Daten aus den Abbildungen 1, 2, 4 und 5 sowie Supplementary Figures S1, S2 und S4 basieren auf von mir etablierten und durchgeführten Experimenten. Dr. Silvia Thöne, Dr. Beate Hagl, Dr. Christof Winter und Prof. Jürgen Ruland führten die ddPCR und deren Analyse durch und interpretierten die Ergebnisse. Sophie Bonnal und Dr. Beate Hagl klonierten die Minigene-Konstrukte und führten die Minigene-Experimente durch (Fig. 3). Dr. Christian Mertes, Dr. Beate Hagl, Prof. Julien Gagneur und Prof. Thomas Meitinger führten die *in silico* Analysen zur kryptischen und kanonischen Splice-Site durch (Fig. 3). Prof. Detlev Schindler führte Radiosensitivitätsversuche mit Fibroblasten der Patienten durch und konnte dadurch die

Pathogenität einer Veränderung im Gen *ATM* ausschließen. Andreas Eberherr führte die Experimente mit den HAP1 ARHGAP32 Knock-out-Zellen durch.

Nach Abschluss aller experimentellen Arbeiten waren Frau Prof. Ellen Renner, Frau Dr. Beate Hagl und ich die Hauptautoren des publizierten Manuskripts. Die geteilte Erstautorenschaft ist durch Frau Dr. Beate Hagls Einsatz bei der Etablierung und Durchführung der ddPCR, der Minigene-Experimente, der Sequenzierung von Immunzellsubpopulationen und die *in silico* Analyse der kryptischen Splice-Site, sowie das gemeinsame Schreiben der finalen Publikation begründet. Alle Autoren beteiligten sich an der Manuskripterstellung und gaben ihr Einverständnis zur Veröffentlichung der finalen Manuskriptversion.

3 Einleitung

Primäre Immundefekte und Gendiagnostik

Die Gruppe der primären Immundefekte (PID) umfasst aktuell über 350 verschiedene, genetisch definierte Erkrankungen (1-5), die mit einer eingeschränkten Entwicklung oder Aktivität des Immunsystems einhergehen. Wie aus Abbildung 1 ersichtlich wird, konnten insbesondere in den vergangenen zehn Jahren durch verbesserte genetische Untersuchungsmöglichkeiten wie dem *Next Generation Sequencing* (NGS) und die gestiegene Wahrnehmung für diese seltenen Erkrankungen eine Vielzahl von Gendefekten die zu PID führen identifiziert werden. Im Gegensatz zur Sanger-Sequenzierung, bei der in einem Versuchsansatz ein definierter Basenabschnitt der DNA amplifiziert wird, werden unter dem Begriff *Next Generation Sequencing* neue Genomanalyse-Verfahren verstanden, bei denen eine sehr große Anzahl von DNA-Molekülen parallel sequenziert wird. Es kommen verschiedene Techniken zum Einsatz, die eine massive, parallele Amplifikation von DNA-Fragmenten in einem Ansatz ermöglichen. Ein Vorteil von NGS liegt somit in der verkürzten Amplifikationsdauer. Es besteht dabei die Möglichkeit einige gezielt ausgewählte Gene, ein gesamtes Exom (*whole exome sequencing*, WES) oder Genom (*whole genome sequencing*, WGS) zu amplifizieren (6).

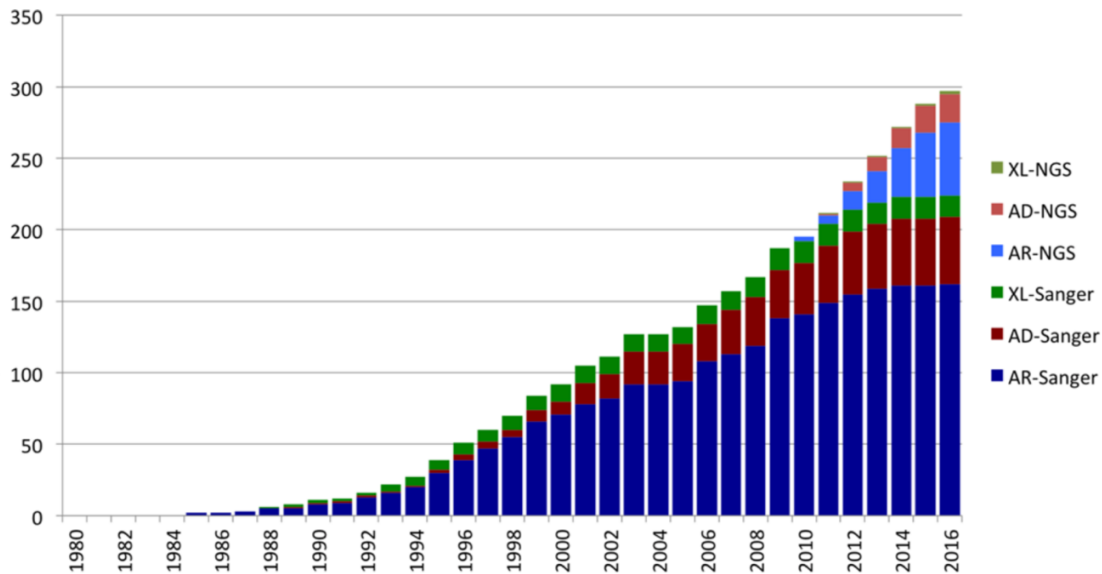


Abb. 1.: Anstieg der mit angeborenen Immundefekten assoziierten Gene (y-Achse) im Verlauf der Jahre (x-Achse). Abkürzungen: AR: autosomal-rezessiv, AD: autosomal-dominant, X: X-chromosomal vererbt. Abb modifiziert nach (6).

Hyper-IgE Syndrome

Hyper-IgE Syndrome (HIES) stellen eine Untergruppe der PID dar und zeichnen sich durch Ekzem, erhöhtes Serum-IgE und rezidivierende Infektionen aus (4, 7-12).

Die Erstbeschreibung 1966 – damals als Job Syndrom – geht auf zwei Patienten mit ungewöhnlich häufigem Auftreten von Abszessen durch *Staphylokokkus aureus* und ekzematöser Haut zurück (13). Die Assoziation mit erhöhtem Serum-IgE prägte 1972 den Begriff „Hyper-IgE Syndrom“ (14). 1999 konnte das Hyper-IgE Syndrom (HIES) als Multisystemerkrankung mit Ekzem, erhöhtem Serum-IgE und rezidivierenden Haut- und Atemwegsinfektionen und einem autosomal-dominantem Erbgang beschrieben werden (15). Klinische Hauptcharakteristika des autosomal-dominanten HIES (AD-HIES) sind, neben erhöhtem Serum-IgE, eine variabel ausgeprägte Eosinophilie sowie ein frühzeitig auftretendes Ekzem, welches sich bereits als ausgeprägtes Neugeborenenekzem präsentieren kann.

Häufiges Zeichen der Immunschwäche sind Superinfektionen der ekzematösen Haut mit *Staphylokokkus aureus* oder *Candida albicans*. Darüber hinaus kommt es zu häufigen Infekten der Atemwege wie Sinusitiden oder Pneumonien durch *Staphylokokkus aureus* oder *Streptokokkus pneumoniae*. In den unteren Atemwegen ist die Ausbildung von Pneumatozelen aufgrund schwerer rezidivierender Atemwegsinfektionen, die ein Reservoir für Erreger sein können, beim AD-HIES beschrieben (16, 17). Ein charakteristisches Aussehen des Gesichts mit rauer Haut, prominenter Stirn, tiefliegenden Augen und breitem Nasenrücken ist bekannt. Zusätzlich kommt es bei einer Vielzahl an Patienten zum Auftreten von pathologischen Frakturen der langen Röhrenknochen, und verlängerter Retention der Milchzähne. Auf Basis dieser distinkten Unterscheidungsmerkmale wurde im Jahr 1999 ein Score, basierend auf klinischen Merkmalen wie Milchzahnpersistenz, Gesamt-IgE und Anzahl der Pneumonien oder Hautabszesse, für die Wahrscheinlichkeit des Vorliegens eines autosomal-dominanten Hyper-IgE Syndroms erarbeitet, der die Diagnose bestätigen sollte und somit frühere Therapien ermöglichen sollte (18).

2004 erfolgte die klinische Erstbeschreibung einer Kohorte mit autosomal-rezessivem Vererbungsmuster, welches als autosomal-rezessives HIES (AR-HIES) definiert wurde (19). Das AR-HIES lässt sich klinisch vom AD-HIES durch andere klinische und laborchemische Merkmale abgrenzen. So sind beim AR-HIES das Auftreten von Virusinfektionen durch Herpesviren (HSV1/2, HHV3) mit generalisiertem Ekzema herpeticatum oder *Molluscum contagiosum* Infektionen charakteristisch. Laborchemisch zeigen AR-HIES-Patienten häufig eine Lymphopenie, erniedrigtes Immunglobulin M und eine ausgeprägte Eosinophilie (12). Des Weiteren zeigen Patienten mit AR-HIES keine skeletalen Auffälligkeiten, Milchzahnpersistenz oder überstreckbare Gelenke. AR-HIES Patienten leiden dagegen häufig unter Allergien und anaphylaktischen Reaktionen gegen Nahrungsbestandteile wie Kuhmilchprotein,

Hühnereiweiß oder Hülsenfrüchte (20). Aufgrund der rezidivierenden und persistierenden Virusinfektionen ist bei AR-HIES das Auftreten von malignen Tumoren häufig (10).

Im Rahmen der Ursachenforschung zu Hyper-IgE Syndromen gelang 2006, ausgehend von einem Patienten mit HIES-Phänotyp mit erhöhtem IgE, Ekzem und Immundefekt die Identifikation von Mutationen im Gen *Tyrosin Kinase 2 (Tyk2)* (21). Kurze Zeit später konnten durch Untersuchungen des JAK-STAT-Signalweges in größeren Kohorten und in einem der erstbeschriebenen Patienten dominant-negative Veränderungen im Gen *STAT3 (Signal transducer and activator of transcription 3)* als Ursache für das autosomal-dominante Hyper-IgE Syndrom (AD-HIES) aufgezeigt werden (7-9, 22). Dieses mutierte Protein hat einen dominant-negativen Effekt auf den STAT3-Signalweg und inhibiert die Aktivität des Wildtyp-Allels durch Bildung von Heterodimeren. In der Folge wird die Signaltransduktion von proinflammatorischen Zytokinen, wie Interleukin 6 oder Interleukin 1b durch STAT3 vermindert und die Differenzierung von TH17-Zellen erschwert, weshalb bei AD-HIES Patienten die TH17-Zellzahlen erniedrigt sind (9, 23). TH17-Zellen und Interleukin-17 spielen eine wichtige Rolle bei der Immunabwehr von extrazellulären Bakterien und Pilzen (insbesondere *Candida albicans*) und somit konnte die Infektanfälligkeit bei AD-HIES gut erklärt werden (24-26).

In einer Patientenkohorte mit dem klinischen Bild eines autosomal-rezessivem Hyper-IgE Syndroms konnten durch gezielte Genuntersuchungen compound-heterozygote und homozygote Mutationen sowie Deletionen im Gen *DOCK8 (Dedicator of Cytokinesis 8)* als Ursache für AR-HIES identifiziert werden (12, 27). Durch die Mutationen kommt es entweder zum Expressions- oder zum Funktionsverlust des DOCK8-Proteins. DOCK8 wirkt, als Mitglied der DOCK180-Proteinfamilie, als ein Steuerelement des Aktin-Zytoskeletts und wird hauptsächlich in Zellen des blutbildenden Gewebes exprimiert, wurde aber auch in Gewebe

von Lunge und Pankreas gefunden (11). DOCK8 trägt als GTP-Austauschfaktor (guanine exchange factor, GEF) zur Aktivierung von Guaninriphosphat-bindenden Proteinen (G-Proteine) wie CDC42 bei und moduliert so Aktin-Polymerisation und das Zytoskelett-Rearrangement. Klinisch kommt es hierdurch zu verringerter T-Zellzahl mit geringem Anteil naiver T-Zellen, unzureichender Formation der immunologischen Synapse und verringerter Antikörperbildung (28).

Therapeutisch stehen für AD-HIES und AR-HIES unterschiedliche Konzepte zur Verfügung. Die Therapie für das AD-HIES besteht derzeit vor allem in konsequenter prophylaktischer antiinfektiver und supportiver Therapie, um Überleben und Lebensqualität möglichst zu verbessern (10, 29). Hämatopoetische Stammzelltransplantationen (HSZT) in AD-HIES sind als Einzelbeschreibungen bekannt (30, 31) und bleiben bisher eine individuelle Entscheidung. Aufgrund der Multisystemerkrankung ist bislang nicht klar ist, ob eine HSZT zum Beispiel auch für die Lungenstrukturveränderungen wie Pneumatozelenbildung hilfreich ist. Wohingegen, aufgrund des schwer ausgeprägten Erkrankungsbildes mit Tendenz zur Bildung maligner Tumore, die möglichst frühe HSZT Therapie der Wahl für DOCK8-HIES ist (10, 29).

Ausblick:

Trotz der Fortschritte in der genetischen Diagnostik ist es derzeit noch nicht gelungen für alle Patienten mit einem Hyper-IgE Syndrom eine genetische Diagnose zu sichern. Diagnostische Schwierigkeiten sind beispielsweise darin begründet, dass mit den gängigen Methoden der Sequenzierung vorrangig das Exom mit kleinen Teilbereichen der angrenzenden Introne, also die codierende DNA untersucht wird. Somit kann zwar eine rasche Aussage über das Vorliegen von Mutationen in diesen Bereichen getroffen werden, jedoch keinerlei Aussage zu den weiter im Intron liegenden, nicht-kodierenden Sequenzen. Diese nicht-kodierenden Sequenzen üben

jedoch in der Funktion als Promotoren, Enhancer oder auch Silencer zum Teil großen Einfluss auf die Regulation der DNA Transkription aus. Neben technisch bedingten Herausforderungen aufgrund großer Datenmenge können auch beispielsweise ein genetisches Mosaik, also Mutationen in nur einem Gewebe, oder Reversionen von Mutationen in schnell teilenden Zellreihen, die molekulargenetische Diagnose und damit die individuelle Therapieentscheidung erschweren.

Zusammenfassend kann festgehalten werden, dass trotz verbesserter genetischer Diagnostik, für die Versorgung der Patienten die Aufmerksamkeit bezüglich der klinischen, PID spezifischen Warnsignale, wie erhöhte Infektanfälligkeit und Infektionen mit protrahiertem oder therapieresistentem Verlauf, weiterhin entscheidend ist. Neben der Basisdiagnostik von Differentialblutbild, Immunglobulinspiegeln im Serum und spezifischer Antikörperbildung kann gegebenenfalls eine weiterführende immunologische Diagnostik hilfreich sein. Nur durch frühzeitige und effektive Therapie sowie Infektionsprophylaxe kann die Entstehung irreversibler Schäden begrenzt werden.

4 Zusammenfassung

Ziel der vorliegenden Arbeit ist es genauere Einblicke in die Vererbung und Pathogenese von Immundefekten aus dem Spektrum der Hyper-IgE Syndrome zu erlangen und so frühzeitig eine molekulargenetische Diagnose zu sichern um eine supportive oder kurative Therapie ermöglichen zu können bevor irreversible Krankheitskomplikationen entstehen.

In der Veröffentlichung „Challenges of genetic counseling in patients with autosomal dominant diseases, such as the hyper-IgE syndrome (STAT3-HIES)“ beschreiben wir drei Kinder mit AD-HIES, die einen gemeinsamen Vater, jedoch zwei unterschiedliche Mütter haben. Als Ursache konnten wir erstmalig die Vererbung einer heterozygoten, dominanten STAT3-Variante als paternales Keimzellmosaik belegen. Autosomal-dominante Veränderungen in *STAT3* sind vorwiegend zufällige Keimbahnveränderungen, sogenannte Spontanmutationen, sodass die Wiederholungswahrscheinlichkeit für gesunde Eltern als gering eingeschätzt wird. Sollte es aber zu gehäuftem Auftreten einer identischen Mutation bei Nachkommen gesunder Eltern kommen zeigt unsere Veröffentlichung auf, dass ein Keimzellmosaik abgeklärt werden sollte, um gezielt genetisch beraten zu können.

In der Arbeit „Somatic alterations compromised molecular diagnosis of DOCK8 hyper-IgE syndrome caused by a novel intronic splice site mutation“ untersuchten wir eine Patientin mit Verdacht auf ein HIES eingehend. Klinisch präsentierte sich die Patientin mit ausgeprägtem Ekzem, rezidivierenden kutanen Superinfektionen, Gedeihstörung und multiplen Nahrungsmittelallergien. Bereits im ersten Lebensjahr litt die Patientin unter einer schweren Pneumonie, die zu Intubation und invasiver Beatmung führte. Auf der Basis der aus der Beatmung folgenden Bronchiolitis obliterans entwickelte sich durch eine *Pseudomonas aeruginosa* Besiedlung ein fibrotischer Umbau der Lunge. Trotz normaler Th17-Zellzahl zeigte sich eine verminderte Stimulierbarkeit von STAT3 auf Interleukin 6 (IL6), nicht aber auf

Interleukin 10 (IL10), hinweisend für einen Defekt in der IL6-STAT3-Achse. DOCK8-Protein war in der Durchflusszytometrie- und Western-Blot-Analyse darstellbar. Ein PID-Genpanel und ein *whole exome sequencing* (WES) blieben ohne Ergebnis zur Klärung der Krankheitsursache. Erst die Untersuchung des gesamten Genoms (*whole genome sequencing*, WGS) und dezidierte Sequenzierung der cDNA von DOCK8 zeigte eine bislang nicht beschriebene Intronvariante, die zu fehlerhaftem Spleißen von DOCK8 führte. Zusätzlich zeigte sich, dass es in Teilen der T-Zellen und nahezu allen natürlichen Killerzellen (NK-Zellen) zu spontanen Reversionen der Intronmutation gekommen ist. Die Zellen mit Reversion hatten somit vermutlich einen relativen Überlebensvorteil und konnten übermäßig expandieren, weshalb es zur Expression von DOCK8-Protein und dem positiven Nachweis in der Durchflusszytometrie und Western-Blot kam. Das defekte STAT3-Signalling ließ sich, nach Ausschluss von Autoantikörpern, durch eine Verschiebung von T-Zelluntergruppen zu, bei der Patientin vorherrschenden, effector memory T-Zellen (Tem) und exhausted effector memory T-Zellen (Temra) erklären, für welche bekannt ist, dass diese eine verminderte IL6-STAT3 Stimulierbarkeit zeigen. Zeitlich parallel zu den Untersuchungen in der Patientin wurde ihre jüngere Schwester geboren, bei der die identische genetische Veränderung gefunden wurde. Für beide Kinder konnte erfolgreich eine Stammzelltransplantation erfolgen, so dass insbesondere die jüngere Schwester vor schwerwiegenden Infektionskomplikationen bewahrt werden konnte.

Zusammenfassend zeigen diese Familien einige Herausforderungen der genetischen und klinischen Aufarbeitung bei Verdacht auf Immundefektsyndrome deutlich auf.

Hoffnung für die noch nicht diagnostizierten Patientinnen und Patienten gibt die Entwicklung hin zur Sequenzierung des gesamten Genoms gekoppelt mit funktionellen Proteinuntersuchungen (Multi-Omics-Verfahren), sodass eine weitere Verbesserung der individuellen Prognose durch frühzeitige Therapien greifbar wird.

5 Summary

The aim of the present study is to obtain detailed insights into the inheritance and pathogenesis of immunodeficiencies like the hyper-IgE syndromes and to ensure a genetic diagnosis in order to enable a supportive and curative therapy before irreversible disease complications arise.

In the publication "Challenges of genetic counseling in patients with autosomal dominant diseases, such as the hyper-IgE syndrome (STAT3-HIES)", we describe three children with AD-HIES, who have one father but two mothers. We were able to show for the first time the inheritance of a heterozygous, dominant-negative STAT3 variant as a paternal germ cell mosaic. Autosomal dominant changes in STAT3 are predominantly random germline changes, so-called spontaneous mutations, so that the probability of recurrence for healthy parents is considered low. However, frequent occurrence of an identical mutation in offspring of healthy parents might be due to a germ cell mosaicism and should be clarified in order to be able to give good genetic counseling as shown in our publication.

In "Somatic alterations compromised molecular diagnosis of DOCK8 hyper-IgE syndrome caused by a novel intronic splice site mutation" we assessed a patient with a suspected HIES in detail. Clinically, the patient presented with pronounced eczema, recurrent cutaneous superinfections, failure to thrive, and multiple food allergies. Already in the first year of life, the patient suffered from severe pneumonia, which led to intubation and invasive ventilation. On the basis of the bronchiolitis obliterans resulting from the respiration, a fibrotic remodeling of the lung developed through a *Pseudomonas aeruginosa* colonization. Despite normal Th17 cell count, decreased stimulation of STAT3 to interleukin 6, but not to interleukin 10, indicated a defect in the IL6-STAT3 axis. DOCK8 protein was present in flow cytometry and western blot analysis. A PID gene panel and whole exome sequencing (WES) analysis identified no cause of

the disease. Only the investigation of the entire genome and the dedicated sequencing of the cDNA of DOCK8 revealed a previously unknown pathogenic intron variant, which led to defective splicing of DOCK8. In addition, it has been shown that parts of the T cells and almost all natural killer cells (NK cells) have spontaneously reversed the intron mutation. The cells with reversion presumably showed a relative survival advantage and were able to expand excessively, resulting in expression of DOCK8 protein and detection in flow cytometry and Western blot. Defective STAT3 signaling, after exclusion of autoantibodies, was shown to be due to a shift of T cell compartments with patient-dominated effector memory T cells (Tem) and exhausted effector memory T cells (Temra) which are known to be less responsive to IL6 stimulation and subsequent STAT3 activation. During the patient's assessment, her younger sister was born, in whom the identical genetic change was found. Both children successfully received a hematopoietic stem cell transplantation (HSCT), with the result that especially in the younger sister serious infectious complications could be prevented.

In summary, these families clearly show some challenges of genetic and clinical workup in suspected immunodeficiency syndromes.

Hope for yet undiagnosed patients arises from the movement towards sequencing of the entire genome coupled with functional protein studies (multi-omics methods), enabling further improvement of the individual prognosis by early therapies.

6 Schriftenverzeichnis

6.1 Originalarbeit: Challenges of genetic counseling in patients with autosomal dominant diseases, such as the hyper-IgE syndrome (STAT3-HIES)

Spielberger BD, Woellner C, Dueckers G, Sawalle-Belohradsky J, Hagl B, Anslinger K, Bayer B, Siepermann K, Niehues T, Grimbacher B, Belohradsky BH, Renner ED. Challenges of genetic counseling in patients with autosomal dominant diseases, such as the hyper-IgE syndrome (STAT3-HIES). *J Allergy Clin Immunol.* 2012 2012 Dec;130(6):1426-8.

This study was supported by the PCIRN (Public Health Agency of Canada–Canadian Institutes for Health Research Influenza Research Network).

Disclosure of potential conflict of interest: G. De Serres received the vaccines used in this study from GlaxoSmithKline and has received grants from GlaxoSmithKline and Sanofi. J. P. Drolet has received payment for lectures/service on speakers' bureaus from Merck and Pfizer. D. Banerjee receives payment from Schering-Plough for short articles that are published online about topics related to allergies. C. Lemire has received payment for lectures/service on speakers' bureaus from Abbott, Merck, and Nestlé. A. Moore has consultant arrangements with Nycomed and has received payment for lectures/service on speakers' bureaus from King Pharmaceuticals Canada and Pfizer. E. S. Chan has received grants and travel support from the Public Health Agency of Canada. D. Stark has received travel support from the University of Laval and the government of Quebec. M. Benoit was employed by Janssen-Ortho and owned stock in Janssen-Ortho and Johnson & Johnson. The rest of the authors declare that they have no relevant conflicts of interest.

REFERENCES

- Lafèche J, Ahmandipour N, Anyoti H, Pless R, Law B. The safety profile of pandemic H1N1 vaccines: reports of adverse events following immunization (AEFI) received by the Public Health Agency of Canada (PHAC), October 2009 through March 2010. *Can J Infect Dis Med Microbiol* 2010;21:223.
- Kurz X, Dommegue F, Slattery J, Segec A, Szmigiel A, Hidalgo-Simon A. Safety monitoring of influenza A/H1N1 pandemic vaccines in EudraVigilance. *Vaccine* 2011;29:4378-87.
- Groupe Central ESPRI. Surveillance des manifestations cliniques inhabituelles survenues après la vaccination contre la grippe A(H1N1) lors de la campagne de masse de l'automne 2009 au Québec. Québec, QC: Ministère de la Santé et des Services sociaux du Québec; 2010.
- Seitz CS, Brocker EB, Trautmann A. Vaccination-associated anaphylaxis in adults: diagnostic testing ruling out IgE-mediated vaccine allergy. *Vaccine* 2009;27:3885-9.
- Liew KW, Crawford N, Tang ML, Buttery J, Royle J, Gold M, et al. Hypersensitivity reactions to human papillomavirus vaccine in Australian schoolgirls: retrospective cohort study. *BMJ* 2008;337:a2642.
- Kelso JM. Adverse reactions to vaccines for infectious diseases. In: Adkinson NF, Middleton E, editors. *Middleton's Allergy: Principles & Practice*. 7th ed. Philadelphia, PA: Mosby/Elsevier; 2009.
- Wood RA, Berger M, Dreskin SC, Setse R, Engler RJ, Dekker CL, et al. An algorithm for treatment of patients with hypersensitivity reactions after vaccines. *Pediatrics* 2008;122:e771-7.
- Wood RA, Setse R, Halsey N. Irritant skin test reactions to common vaccines. *J Allergy Clin Immunol* 2007;120:478-81.
- Sugai K, Shiga A, Okada T, Iwata T, Ogura H, Maekawa K, et al. Dermal testing of vaccines for children at high risk of allergies. *Vaccine* 2007;25:3454-63.

Available online September 6, 2012.
<http://dx.doi.org/10.1016/j.jaci.2012.07.019>

Challenges of genetic counseling in patients with autosomal dominant diseases, such as the hyper-IgE syndrome (STAT3-HIES)

To the Editor:

Heterozygous mutations in the transcription factor signal transducer and activator of transcription 3 (*STAT3*) cause autosomal dominant hyper-IgE syndrome (HIES), which presents with *Staphylococcus aureus* skin abscesses, pneumonias with pneumatocele formation, mucocutaneous candidiasis, and eczema with increased serum IgE levels.¹⁻³ Here we report a family with 3 children affected by autosomal dominant HIES, suggesting genetic inheritance (Fig 1). Grandparents and both mothers (individuals I.1 and I.3) do not show any clinical findings of STAT3-HIES. The common father (individual I.2) of the 3 children is healthy except for mild atopic periorbital eczema since childhood. He has normal serum IgE levels (11.3 IU/mL), had 1 sinusitis, and had a tonsillectomy because of chronic inflammation.

The index patient is the 10-year-old daughter (individual II.1) of I.1 and I.2, who was born 2 weeks preterm after an

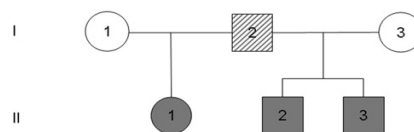


FIG 1. Pedigree of the family. The index patient (subject II.1), as well as her 2 half brothers (individuals II.2 and II.3), are shown as *solid symbols*, which indicate affected subjects. *Open symbols* present unaffected subjects with the wild-type sequence (individuals I.1 and I.3), whereas the *striped symbol* reflects the mosaicism of individual II.2. *Squares* indicate male individuals, and *circles* indicate female individuals.

unremarkable pregnancy. At 5 months of age, she started experiencing eczematous dermatitis, which spread from the head to the shoulders. She had recurrent oral and diaper dermatitis, otitis media, urinary tract infections, bronchitis, and pneumonia, some of which required intravenous antibiotic treatment. At 4 years of age, she was started on prophylactic antibiotic treatment with cefuroxime. Failure to shed primary teeth, increased serum IgE levels (9.716 IU/mL; value for age, <90 IU/mL), onychomycosis, recurrent bacterial infections of the skin and airways, hyperextensible joints, and characteristic facies were additional findings indicative of STAT3-HIES. Genomic analysis was completed at the age of 6 years, and the heterozygous *STAT3* hotspot mutation R382Q was identified. Radiography at 10 years of age revealed scoliosis of the lumbar and thoracic spine, with no signs of pneumatoceles or bronchiectasis.

The 6-year-old son (individual II.2.) of individuals I.2 and I.3 was born at full term after an unremarkable pregnancy. He had a newborn rash and started experiencing recurrent *Staphylococcus aureus* infections all over his skin. At 1 year of age, he had an abscess at the foreskin requiring surgery and intravenous antibiotic treatment. At the age of 5 years, persistent oral thrush required treatment with amphotericin B. He has no history of pathologic bone fractures, scoliosis, or hyperextensible joints, as seen in patients with STAT3-HIES, but has contractures of the tendons of 3 fingers. He has an increased serum IgE level (738 IU/mL at age 5 years; value for age, <90 IU/mL).

His 4-year-old brother (individual II.3) presented with eczema and recurrent respiratory tract infections beginning in early infancy. Recurrent otitis media required antibiotic treatment until the placement of tympanostomy tubes. Antibiotic prophylaxis was started at 3.5 years of age. Despite recurrent respiratory tract infections, he has not developed chronic lung changes, such as pneumatoceles. Scoliosis of the cervical spine was confirmed by means of chest radiography. His serum IgE level is increased (266 IU/mL at age 4 years; value for age, <60 IU/mL).

To confirm STAT3-HIES, sequencing of the gene *STAT3* was performed by using the Sanger technique with genomic DNA (gDNA) extracted from peripheral blood, as described previously.⁴ The heterozygous mutation c.1145G>A, p.R382Q in exon 13 of the *STAT3* gene, was found in the 3 children (Fig 2), whereas the parents (individuals I.1, I.2, and I.3) had the wild-type sequence for exon 13.

Because it did not seem likely that all 3 children had independent and sporadic identical mutations, gDNA from the semen and oral mucosa of individual I.2 was extracted with a Biorobot EZ1 forensic card (Qiagen, Hilden, Germany).⁵ The mutation was not found in the oral mucosa gDNA, but the heterozygous R382Q

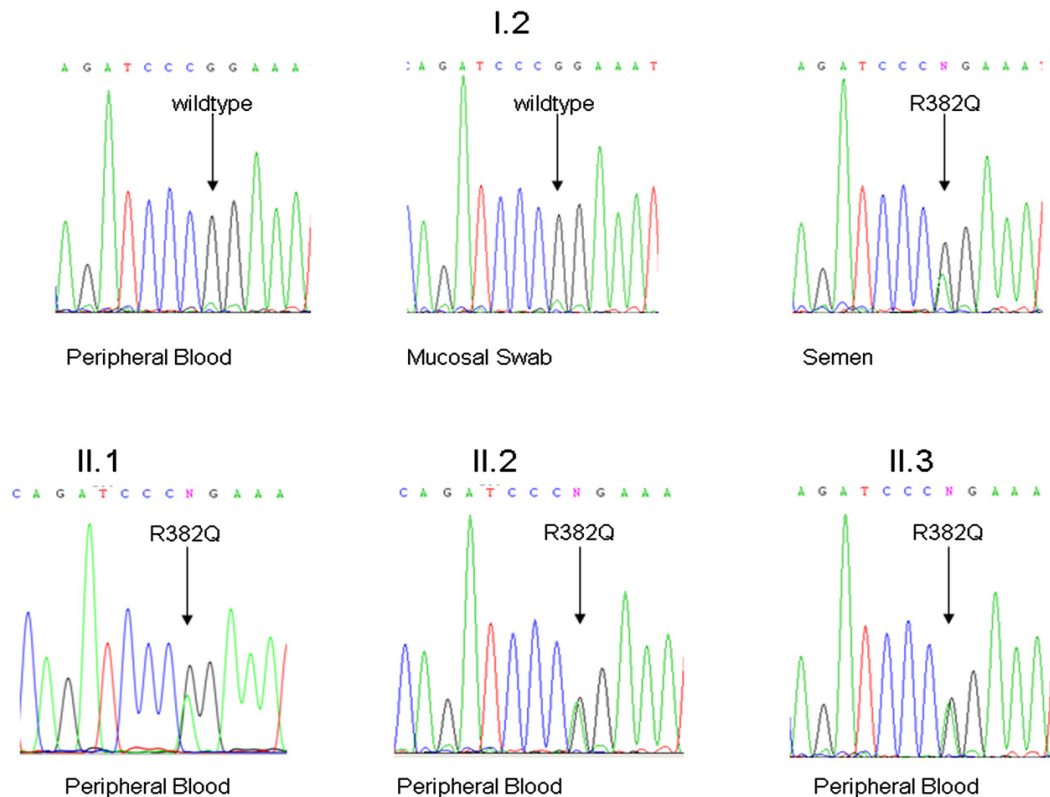


FIG 2. Mutation analysis of affected family members. Mutation analysis of individual II.2 shows the wild-type sequence of gDNA isolated from peripheral blood and mucosal cells. The gDNA of individual II.2 isolated from semen carries the heterozygous *STAT3* mutation c.1145G>A, R382Q, which has been identified in all his clinically affected offspring (individuals II.1-II.3).

mutation of the gene *STAT3* was identified in the genetic material extracted from the semen (Fig 2).

To show the functional consequence of the identified *STAT3* mutation, peripheral mononuclear cells were stimulated with phorbol 12-myristate 13-acetate/ionomycin to assess the T_H17 cell numbers, as previously described.⁴ T_H17 cell counts are known to be significantly decreased in patients with *STAT3*-HIES,^{4,6} and indeed, they were diminished in subjects II.1, II.2, and II.3 (0.03%, 0.07%, and 0.15% T_H17 cells of $CD4^+$ cells; value in healthy control individuals, >0.2% $CD4^+$ cells), whereas subject I.2, with the wild-type *STAT3* sequence in peripheral blood, had normal values (1.40% $CD4^+$ cells).

As with other autosomal dominant diseases, *STAT3*-HIES in children with unaffected parents is suggested to be a result of spontaneous *in utero* mutations. Thus the risk of subsequent offspring being affected with the same condition is thought to be negligible. However, the fact that individual I.2 has healthy parents and 3 children with the complete clinical spectrum of *STAT3*-HIES caused by the identical heterozygous *STAT3* mutation (R382Q) involving subjects I.1 and I.3 suggests a paternal germline mosaicism.

Mosaicism is present if 1 individual has 2 or more cell lines with a different genotype that developed from a single fertilized homogeneous zygote.⁷ Because only the germ cells of the semen and not the somatic cells (oral mucosa and PBMCs) are mutated, subject I.2 is healthy but can pass down the mutation to his offspring (individuals II.1, II.2, and II.3) with variable penetration. The cause is usually a mutation that occurred in an early stem cell that gave rise to the gonadal tissue. The maximum amount of affected germ cells is 50% and is dependent on the developmental stage at which the mutation occurred.⁷

This family illustrates the complexity of genetic counseling in cases of autosomal dominant inherited diseases. Sequencing the gDNA of the parents' peripheral blood might not be sufficient in patients with *STAT3*-HIES to rule out an increased risk for additional affected children. An increased risk of penetrance caused by an unknown mosaicism in germ cells has to be considered. Zlotogora et al⁷ stated in 1998 that there are too few data on carriers of germline mosaicism and its recognition in genetic diseases. Only a few germline mosaicisms have been observed in patients with primary immunodeficiencies, such as Wiskott-Aldrich syndrome, X-linked

severe combined immunodeficiency, DiGeorge syndrome, and severe congenital neutropenia.⁸⁻¹¹ This report of a germline mosaicism in an additional autosomal dominant primary immunodeficiency should further raise awareness of this condition.

Overall, we recommend informing family members of patients with STAT3-HIES about the possibility of mosaicism. Furthermore, genetic testing of every newborn in families with known members carrying STAT3 mutations is suggested to ensure the diagnosis of STAT3-HIES early in life. Only an early diagnosis of STAT3-HIES allows initiation of the right treatment necessary for limiting complications caused by infections and to benefit the quality of life of the individual patient.

We thank the patients and their family for their participation, primary care provider Dr Möller for patient care, Dr Sarah Andrews for critical review of the manuscript, and Irmgard Eckerlein and Mayumi Hoffmann for technical assistance and performing flow cytometry.

Benedikt D. Spielberger^a
Cristina Woellner, MSc^b
Gregor Dueckers, MD^c
Julie Sawalle-Belohradsky^a
Beate Hagl, PhD^a
Katja Anslinger, MD^d
Birgit Bayer^d
Kathrin Siepermann, MD^c
Tim Niehues, MD^c
Bodo Grimbacher, MD^b
Bernad H. Belohradsky, MD^a
Ellen D. Renner, MD^a

From ^athe University Children's Hospital and ^dthe Institute of Legal Medicine, Ludwig-Maximilians-Universität, Munich, Germany; ^bthe Centre of Chronic Immunodeficiency (CCI), University Medical Center Freiburg and University of Freiburg, Freiburg, Germany; and ^cChildren's Hospital, Helios Kliniken, Krefeld, Germany. E-mail: Ellen.Renner@med.lmu.de.

Supported by the Kindness for Kids Foundation grant (to J.S.-B.), the German Research Foundation (DFG RE2799/3-1), the Fritz-Thyssen research foundation grant (Az. 10.07.1.159), the LMU Munich FoFoLe grant #680/658 (to E.D.R.), and the German Federal Ministry of Education and Research (BMBF 01 EO 0803) (to B.G.). Data included in this publication are part of a medical thesis at the School of Medicine, Ludwig Maximilian University Munich (BDS).

Disclosure of potential conflict of interest: B. Grimbacher has received payment for a lecture from the American Academy of Allergy, Asthma & Immunology and has received research support from the German Federal Ministry of Education and Research. The rest of the authors declare that they have no relevant conflicts of interest.

REFERENCES

- Grimbacher B, Holland SM, Gallin JI, Greenberg F, Hill SC, Malech HL, et al. Hyper-IgE syndrome with recurrent infections—an autosomal dominant multisystem disorder. *N Engl J Med* 1999;340:692-702.
- Minegishi Y, Saito M, Tsuchiya S, Tsuge I, Takada H, Hara T, et al. Dominant-negative mutations in the DNA-binding domain of STAT3 cause hyper-IgE syndrome. *Nature* 2007;448:1058-62.
- Holland SM, DeLeo FR, Elloumi HZ, Hsu AP, Uzel G, Brodsky N, et al. STAT3 mutations in the hyper-IgE syndrome. *N Engl J Med* 2007;357:1608-19.
- Schimke LF, Sawalle-Belohradsky J, Roessler J, Wollenberg A, Rack A, Borte M, et al. Diagnostic approach to the hyper-IgE syndromes: immunologic and clinical key findings to differentiate hyper-IgE syndromes from atopic dermatitis. *J Allergy Clin Immunol* 2010;126:611-7, e1.
- Anslinger K, Bayer B, Rolf B, Keil W, Eisenmenger W. Application of the BioRobot EZ1 in a forensic laboratory. *Leg Med (Tokyo)* 2005;7:164-8.
- Milner JD, Brenchley JM, Laurence A, Freeman AF, Hill BJ, Elias KM, et al. Impaired T(H)17 cell differentiation in subjects with autosomal dominant hyper-IgE syndrome. *Nature* 2008;452:773-6.
- Zlotogora J. Germ line mosaicism. *Hum Genet* 1998;102:381-6.
- Arveiler B, de Saint-Basile G, Fischer A, Griscelli C, Mandel JL. Germ-line mosaicism simulates genetic heterogeneity in Wiskott-Aldrich syndrome. *Am J Hum Genet* 1990;46:906-11.
- Puck JM, Pepper AE, Bedard PM, Laframboise R. Female germ line mosaicism as the origin of a unique IL-2 receptor gamma-chain mutation causing X-linked severe combined immunodeficiency. *J Clin Invest* 1995;95:895-9.
- Sandrin-Garcia P, Macedo C, Martelli LR, Ramos ES, Guion-Almeida ML, Richieri-Costa A, et al. Recurrent 22q11.2 deletion in a sibship suggestive of parental germline mosaicism in velocardiofacial syndrome. *Clin Genet* 2002;61:380-3.
- Newburger PE, Pindyck TN, Zhu Z, Bolyard AA, Aprikyan AA, Dale DC, et al. Cyclic neutropenia and severe congenital neutropenia in patients with a shared ELANE mutation and paternal haplotype: evidence for phenotype determination by modifying genes. *Pediatr Blood Cancer* 2010;55:314-7.

Available online September 13, 2012.
<http://dx.doi.org/10.1016/j.jaci.2012.07.030>

LRBA gene deletion in a patient presenting with autoimmunity without hypogammaglobulinemia

To the Editor:

Primary immunodeficiencies are a highly heterogeneous group of genetic disorders caused by Mendelian mutations in >150 immune-related genes.¹ Primary immunodeficiencies manifest as severe and/or disseminated recurrent infections and may also have autoimmune manifestations.

We studied a female patient P1 of Pakistani origin who presented at the age of 4 years with a generalized lymphadenopathy, splenomegaly, neutropenia (range, 0.05-0.28 × 10⁹/L), and thrombocytopenia (platelet count, 20-40 × 10⁹/L). A lymph node biopsy showed reactive changes, bone marrow aspirate was unremarkable, and antineutrophil antibodies were present. She also had chronic diarrhea associated with an autoimmune enteropathy, characterized by duodenal villous atrophy and large bowel lymphocytic infiltration on biopsy. Her initial immunology workup found only raised IgG levels (22.6 g/L), raised inflammatory markers, and a low number of natural killer cells (0.00-0.02). Lymphocyte subsets, double-negative T cells, T-cell proliferation assays, IgA (1.33 g/L), IgM (1.43 g/L), tetanus vaccine responses, and a nitroblue tetrazolium test were normal (Table I). P1 had no significant history of infections except for a psoas abscess associated with chronic neutropenia. Over time she manifested growth failure and developed new autoimmune features, including an episode of erythema nodosum, transient arthritis of both feet, and recurrent hemolytic anemia. As a result, she received several courses of steroids, rituximab (with prophylactic immunoglobulin replacement), and mycophenolate mofetil. Five years after initial presentation, after multiple courses of rituximab, she developed recurrent infections (*Streptococcus pneumoniae* facial cellulitis, *Streptococcus pneumoniae* sepsis, and *Haemophilus influenzae* empyema) after withdrawal of immunoglobulin therapy. Although both her CD19⁺ B cells and IgG level were normal, further investigation found a new-onset antibody deficiency with absent vaccine responses (Table I). Because of further chest symptoms, despite recommencing immunoglobulin replacement, a chest computed tomographic scan was performed that showed extensive lung infiltration. Lung biopsy showed a florid diffuse lymphoid interstitial infiltrate that consisted of a mixture of CD3⁺ T and CD20⁺ B cells, with scattered lymphoid follicles, particularly around airways. No granulomata were seen, and stains for bacteria, fungi, and mycobacteria, as well as *in situ* hybridisation for EBV, were negative.

Patient P1 was born to a consanguineous marriage of first cousins. Therefore, we hypothesized that her disease was caused

6.2 Originalarbeit: Somatic alterations compromised molecular diagnosis of DOCK8 hyper-IgE syndrome caused by a novel intronic splice site mutation

Beate Hagl*, **Benedikt D Spielberger***, Silvia Thoene, Sophie Bonnal, Christian Mertes, Christof Winter, Isaac J. Nijman, Shira Verduin, Andreas C. Eberherr, Anne Puel, Detlev Schindler, Jürgen Ruland, Thomas Meitinger, Julien Gagneur, Jordan S. Orange, Marielle E. van Gijn, Ellen D. Renner. Somatic alterations compromised molecular diagnosis of DOCK8 hyper-IgE syndrome caused by a novel intronic splice site mutation. *Sci Rep.* 2018 Nov 13;8(1):16719. doi: 10.1038/s41598-018-34953-z.

*shared first author, contributed equally.

SCIENTIFIC REPORTS

OPEN Somatic alterations compromised molecular diagnosis of DOCK8 hyper-IgE syndrome caused by a novel intronic splice site mutation

Received: 25 June 2018

Accepted: 24 October 2018

Published online: 13 November 2018

Beate Hagl^{1,2}, Benedikt D. Spielberger^{1,2}, Silvia Thoene^{3,4,5}, Sophie Bonnal^{6,7}, Christian Mertes⁸, Christof Winter^{3,4,5}, Isaac J. Nijman⁹, Shira Verduin⁹, Andreas C. Eberherr¹, Anne Puel^{10,11,12}, Detlev Schindler¹³, Jürgen Ruland^{3,4,5,14}, Thomas Meitinger¹⁵, Julien Gagneur^{8,16}, Jordan S. Orange^{17,18,19}, Marielle E. van Gijn⁹ & Ellen D. Renner^{1,2,20}

In hyper-IgE syndromes (HIES), a group of primary immunodeficiencies clinically overlapping with atopic dermatitis, early diagnosis is crucial to initiate appropriate therapy and prevent irreversible complications. Identification of underlying gene defects such as in *DOCK8* and *STAT3* and corresponding molecular testing has improved diagnosis. Yet, in a child and her newborn sibling with HIES phenotype molecular diagnosis was misleading. Extensive analyses driven by the clinical phenotype identified an intronic homozygous *DOCK8* variant c.4626 + 76 A > G creating a novel splice site as disease-causing. While the affected newborn carrying the homozygous variant had no expression of *DOCK8* protein, in the index patient molecular diagnosis was compromised due to expression of altered and wildtype *DOCK8* transcripts and *DOCK8* protein as well as defective *STAT3* signaling. Sanger sequencing of lymphocyte subsets revealed that somatic alterations and reversions revoked the predominance of the novel over the canonical splice site in the index patient explaining *DOCK8* protein expression, whereas defective *STAT3* responses in the index patient were explained by a T cell phenotype skewed towards central and effector memory T cells. Hence, somatic alterations and skewed immune cell phenotypes due to selective pressure may compromise molecular diagnosis and need to be considered with unexpected clinical and molecular findings.

¹Chair and Institute of Environmental Medicine, UNIKA-T, Technical University of Munich and Helmholtz Zentrum Munich, Munich/Augsburg, Munich, Germany. ²University Children's Hospital, Dr. von Haunersches Kinderspital, Ludwig Maximilian University, Munich, Germany. ³Institute of Clinical Chemistry and Pathobiochemistry, Klinikum rechts der Isar, Technical University of Munich, Munich, Germany. ⁴German Cancer Consortium (DKTK), partner site Munich, Munich, Germany. ⁵German Cancer Research Center (DKFZ), Heidelberg, Germany. ⁶Centre for Genomic Regulation (CRG), The Barcelona Institute of Science and Technology, Dr. Aiguader 88, Barcelona, 08002, Spain. ⁷Universitat Pompeu Fabra (UPF), Barcelona, Spain. ⁸Department of Informatics, Technical University of Munich, Garching, Germany. ⁹Department of Genetics, University Medical Center Utrecht, Utrecht, The Netherlands. ¹⁰Laboratory of Human Genetics of Infectious Diseases, Necker Branch, Necker Medical School, Paris, France. ¹¹Paris Descartes University, Sorbonne Paris Cité, Institut Imagine, Paris, France. ¹²St Giles Laboratory of Human Genetics of Infectious Diseases, Rockefeller Branch, Rockefeller University, New York, NY, USA. ¹³Department of Human Genetics, University of Würzburg, Würzburg, Germany. ¹⁴German Center for Infection Research (DZIF), partner site Munich, Munich, Germany. ¹⁵Institute of Human Genetics, Technical University of Munich and Helmholtz Zentrum Munich, Neuherberg, Germany. ¹⁶Quantitative Biosciences Munich, Gene Center, Department of Biochemistry, Ludwig Maximilian University, Munich, Germany. ¹⁷Center for Human Immunobiology of Texas Children's Hospital/ Department of Pediatrics, Baylor College of Medicine, Houston, TX, USA. ¹⁸Department of Pediatrics, Division of Immunology, Allergy, and Rheumatology, Baylor College of Medicine, and Texas Children's Hospital, Houston, TX, USA. ¹⁹Department of Pediatrics, Baylor College of Medicine, and Texas Children's Hospital, Houston, TX, USA. ²⁰Hochgebirgsklinik and Christine-Kühne-Center for Allergy Research and Education (CK-Care), Davos, Switzerland. Beate Hagl and Benedikt D. Spielberger contributed equally. Correspondence and requests for materials should be addressed to E.D.R. (email: ellen.renner@tum.de)

Patients with primary immunodeficiencies (PIDs), such as hyper-IgE syndromes (HIES), have benefited tremendously from clinical classifications and the discovery of underlying gene defects and corresponding molecular testing. HIES are rare immunodeficiencies characterized by eczema, elevated serum IgE levels, eosinophilia and recurrent infections; and depending on the underlying genetic defect, additionally persistent primary teeth, allergic findings, lymphopenia or low Th17 cell counts^{1–7}. All HIES entities overlap significantly with more common diseases, particularly severe forms of atopic dermatitis. Hence, prior to the possibility of molecular testing and due to low awareness of HIES, diagnosis was often delayed until severe complications, particularly irreversible lung changes, have impacted patients' quality of life.

The identification of genes causing HIES enabled diagnostic blood testing of low Th17 cell counts and reduced STAT3 phosphorylation in STAT3-HIES^{8,9}, or lack of DOCK8 protein expression in DOCK8-HIES¹⁰. The improved understanding of the immunopathology resulted in treatment optimization^{1–4}, such as the benefit of immunoglobulin substitution therapy in addition to rigorous antibiotic treatments due to the discovered impaired adaptive immunity^{5,11} and the consensus of early hematopoietic stem cell transplantation (HSCT) as treatment of choice in HIES caused by DOCK8 deficiency (DOCK8-HIES)^{11–13}.

With the knowledge that early diagnosis often determines the disease outcome, targeted next-generation sequencing (NGS) has become a cost-efficient tool in PID diagnostics^{14,15}. Due to the rapidly increasing number of newly defined monogenic PIDs molecular PID diagnostics already needs to cover over 350 genes and targeted NGS approaches are limited to a pre-defined set of disease-causing genes^{15,16}. Therefore, whole exome sequencing (WES) and whole genome sequencing (WGS) analyses are starting to replace targeted approaches¹⁵.

The experience of the following family shows how somatic alterations complicated molecular diagnosis and how the close interplay of clinical, immunological, molecular, and bioinformatic diagnostic approaches identified a genetically determined disease.

Results

Clinical and immunological presentation. The index patient (patient II.2) is the second child of healthy first-degree cousins (Fig. 1a); term born with 2860 g (7th percentile) and 34 cm head circumference (25th percentile) after uneventful pregnancy. Recurrent upper and lower respiratory infections started at 2 months, including a fulminant pneumonia, requiring intubation and ventilation resulting in bronchiolitis obliterans at 6 months of age. Recurrent infections led to additional chronic lung changes with bronchiectasis formation and *Pseudomonas aeruginosa* positive lung specimen following frequent exacerbations (Fig. 1b). She developed eczema at 4 months with generalized eczema herpeticum at 12 months of age. Several flares of eczema herpeticum followed, including a herpes simplex blepharitis at around 8 years of age. There were repeated *Molluscum contagiosum* and mucocutaneous *Candida* infections as well as recurrent onychomycosis. She developed multiple specific IgE positive food allergies to milk, eggs, soy, and peanuts; at 12 months of age she suffered an anaphylactic reaction to lentils. Her growth started to slow to the 3rd percentile at 6 months of age and dropped further with significant growth retardation, malnutrition, and iron deficient anemia.

At 3.5 years of age she was referred for PID evaluation. HIES was suspected due to elevated serum IgE (max. value 30434 IU/ml), eosinophilia (max. value 9100 cells/μl), chronic eczema, and recurrent bacterial, fungal, and viral infections, particularly of skin and lungs. Except for hyperextensible joints, she had no other skeletal findings associated with STAT3-HIES. The overall clinical presentation was in-between STAT3- and DOCK8-HIES with 48 points in the NIH-HIES score¹⁷, which sums up findings of STAT3-HIES and is considered predictive for HIES above 40 points.

Immunological work-up revealed high IgE, IgG, and IgA levels, and low to normal IgM levels (Fig. 1c). Mainly normal or high total lymphocyte and NK cell counts with high eosinophil counts were measured (Fig. 1d). Memory B cell counts affecting total, switched and unswitched memory B cells were low. Absolute numbers of total T cells, T helper cells, and cytotoxic T cells were within normal range, except for individual low and high values. Considering the patient's young age, her T cell subsets showed a shift towards a memory phenotype with low percentages of naïve T cells (CCR7⁺CD45RA⁺) and high percentages of effector memory T cells (CCR7⁻CD45RA⁻) in CD4⁺ and CD8⁺ T cells and CD8⁺ T_{EMRA} cells (CCR7⁻CD45RA⁺) (Fig. 1e). Th17 cell counts were normal on two time-points with 0.32% and 0.23% of CD4⁺ cells (normal value: >0.20% of CD4⁺ cells). Lymphocyte stimulation tests assessing proliferation by [³H]thymidine uptake had partially reduced response to mitogens such as Phytohaemagglutinin, OKT3, Concanavalin A and Pokeweed mitogen and markedly reduced reactions to an antigen mixture of Tetanus and Diptheria toxoid antigen (data not shown).

Since recurrent infections and severe failure to thrive were not controlled by intensive antibacterial, -viral and -fungal treatment, the patient was referred again at 8 years of age. When the family ultimately agreed to HSCT, she received donor cells of her mother at 8 years of age. After an uneventful HSCT, her general health condition progressed over the next months with significant improvement of eczema and skin infections and restart of weight- and height-gain. Lymphocyte stimulation test to mitogens as well as B and T cell compartments, including naïve T cells, normalized within the first year after HSCT except for a shift towards cytotoxic T cells. Initially recurrent lung infections remained unchanged, most likely due to the bronchiolitis obliterans resulting from the severe infection at 6 months of age. Three years after HSCT, the frequency of respiratory infections has improved while continuous antibiotic and inhalation treatment are still required. Food allergies to milk, egg, and nuts were still present.

Shortly after HSCT of patient II.2, a third child (patient II.3) was born (3790 g of weight; 77th percentile; 36.5 cm head circumference; 89th percentile). Within the first months of age, she developed eczema, hard to control skin infections, and chronic otitis externa. Except for slightly elevated serum IgE (initially 18.2 IU/ml; max. value 1532 IU/ml at 7 months) and eosinophilia, she presented with lymphocyte counts and proliferation unremarkable for age (data not shown). Also NK, T and B cell counts, including subpopulations and IgG, IgA, and IgM serum were unremarkable for age (Fig. 1c–e). At 8 months of age, she received HSCT from a healthy

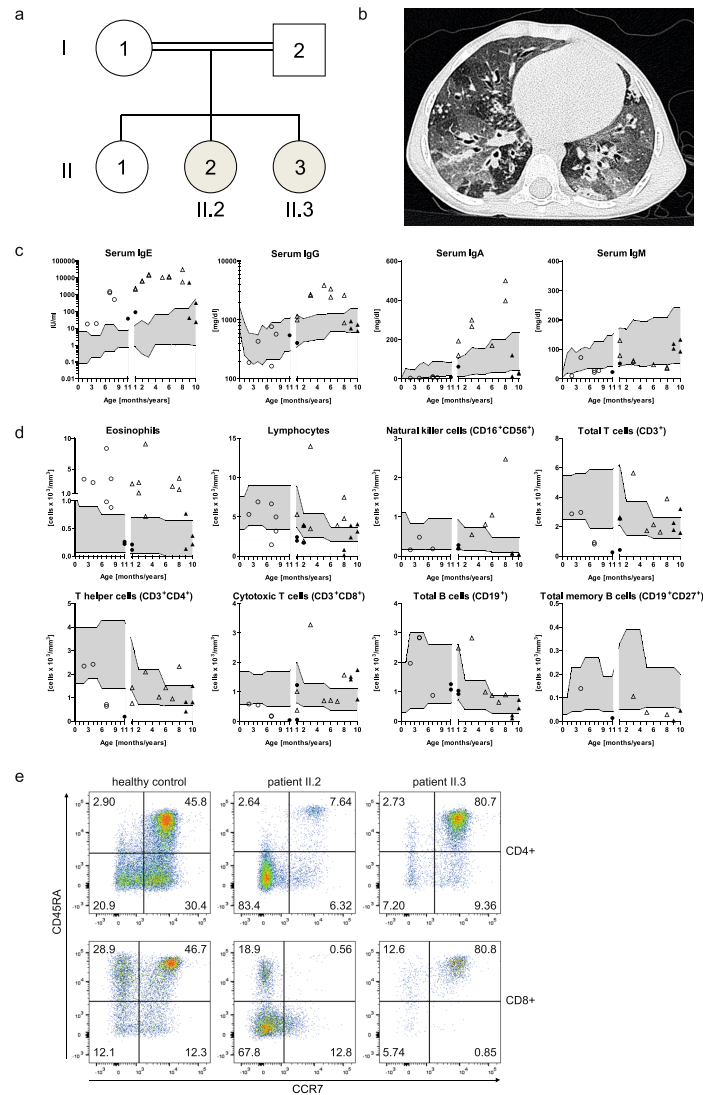


Figure 1. Pedigree, clinical and immunologic presentation of the two affected siblings. (a) Pedigree of the investigated consanguineous family of the two affected siblings: II.2: index patient; II.3: second affected child. (b) Chest CT scan of patient II.2 at 3.5 years of age with areas of ground glass opacities, air trapping, multiple irregular nodular opacities (tree-in-bud sign), and bilateral bronchiectasis representing lung parenchyma destruction. (c) Serum immunoglobulin levels, (d) absolute numbers of eosinophil, lymphocyte and lymphocyte subsets of patient II.2 (triangles) and patient II.3 (circles) before (open symbols) and after HSCT (black filled symbols) compared to age-related normal range (gray filled area). (e) Representative flow cytometric plots showing CD4⁺ and CD8⁺ T cell subsets assessed by CCR7 and CD45RA expression in patient II.2 and patient II.3 compared to a healthy control. Percentages of naïve T cells (CCR7⁺CD45RA⁺), central memory T cells (CCR7⁺CD45RA⁻), effector memory T cells (CCR7⁻CD45RA⁻) and T_{EMRA} cells (CCR7⁻CD45RA⁺) of CD4⁺ or CD8⁺ T cells are indicated by numbers in the respective quadrant.

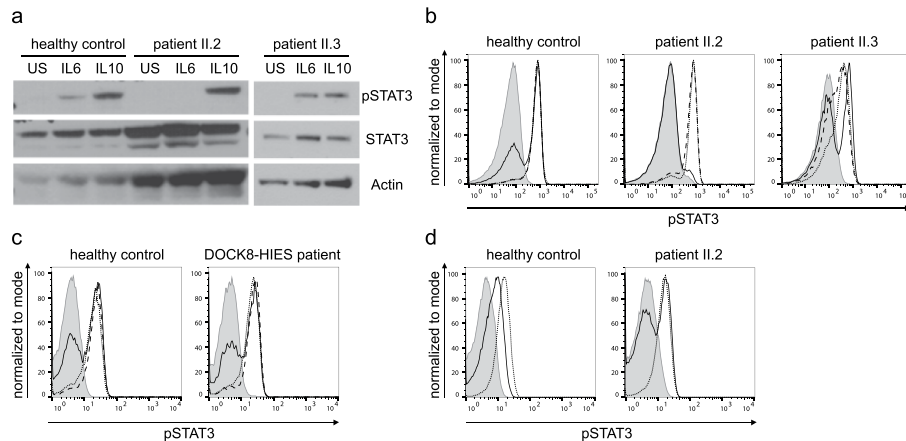


Figure 2. STAT3 phosphorylation analysis after stimulation. **(a)** Western blot analysis of whole cell lysates of PBMCs, unstimulated or 20 min. stimulated with 200 ng/ml IL6 or IL10. Expression of STAT3 phosphorylated at Y705 (pSTAT3) and total STAT3 (STAT3) of the two affected siblings and a healthy control was assessed; Actin as loading control. **(b)** Representative flow cytometric analysis showing diminished Y705-STAT3 phosphorylation after 20 min. stimulation with 200 ng/ml IL6 (solid line) versus unremarkable results after stimulation with 20 ng/ml IL10 (dotted line) and 10 ng/ml IL21 (dashed line) in lymphocytes of patient II.2 compared to unremarkable results in patient II.3 and a healthy control; filled gray area: unstimulated lymphocytes. **(c)** Flow cytometric analysis showing Y705-STAT3 phosphorylation after 20 min. stimulation with 20 ng/ml IL6 (solid line) or IL10 (dotted line) and 10 ng/ml IL21 (dashed line) comparable to healthy control in lymphocytes of one (representative of four) DOCK8-HIES patient. **(d)** Restored STAT3 phosphorylation after IL6 stimulation (solid line) in patient II.2 15 months after HSCT compared to unstimulated (filled gray area) and IL10-stimulated (dotted line) lymphocytes.

unrelated donor. So far, she has developed completely normal without eczema, skin or unusual respiratory infections more than two years after HSCT.

STAT3 signaling analyses. Patient II.2 showed diminished Y705-STAT3 phosphorylation in PBMCs after IL6 stimulation, yet not after IL10 or IL21 stimulation by western blot and flow cytometric analysis (Fig. 2a,b). There was no altered STAT3 phosphorylation in lymphocytes of patient II.3 and four molecularly-defined DOCK8-HIES patients compared to healthy controls (Fig. 2a–c). Slightly decreased STAT3 phosphorylation in lymphocytes of patient II.3 compared to healthy controls was seen in some flow cytometric experiments (Fig. 2b) but overall similar to the range observed in healthy controls and not as clearly reduced as seen in patient II.3. The STAT3 signaling defect in patient II.2 was restricted to immune cells, since STAT3 phosphorylation after IL6 stimulation in patient's fibroblasts was comparable to control fibroblasts. We ruled out IL6-, IL6-receptor (IL6R) and gp130-autoantibodies as cause of the STAT3 signaling defect by multiplex analyses with serum antibody concentrations below or comparable to levels found in control sera. Furthermore, pre-incubation of PBMCs of a healthy control with serum of patient II.2 had no effect on IL6- and IL10-induced STAT3 phosphorylation (Supplementary Fig. S1). Similarly to other immunological alterations, STAT3 phosphorylation normalized in lymphocytes of patient II.2 within one year after HSCT (Fig. 2d).

Genetic analyses. In search of the genetic cause of the underlying PID of patient II.2, we performed a previously described PID targeted NGS approach¹⁴, including *STAT3* and *DOCK8*. A homozygous single nucleotide variant in the *ATM* gene (c.1010 G > A, p.R337H) was detected and ruled-out to be disease-causing by normal radiation sensitivity testing of fibroblasts of patient II.2 and later a normal *ATM* sequence of patient II.3. Next, we completed WES analysis in patient II.2 and identified a homozygous alteration in *ARHGAP32* (c.6038 G > A, p.R2013H). This alteration was considered disease-causing because ARHGAP32 is a GTPase-activating protein (GAP)¹⁸ and another GAP, called MgcRacGAP, has been associated with IL6-induced STAT3 phosphorylation in human and murine *in vitro* models^{19,20}. However, STAT3 phosphorylation was not restored by overexpressing wildtype ARHGAP32 in patient cells and IL6-induced STAT3 phosphorylation in an ARHGAP32 knock-out HAP1 cell line was intact (Supplementary Fig. S2).

WGS of patient II.2 and the healthy parents and a recessive model approach analysis did not lead to any additional candidates. *De novo* variants analysis of the WGS data revealed four putative candidate variants, which were excluded due to their intergenic location or their location of more than 9 kb up- or downstream of adjacent exons.

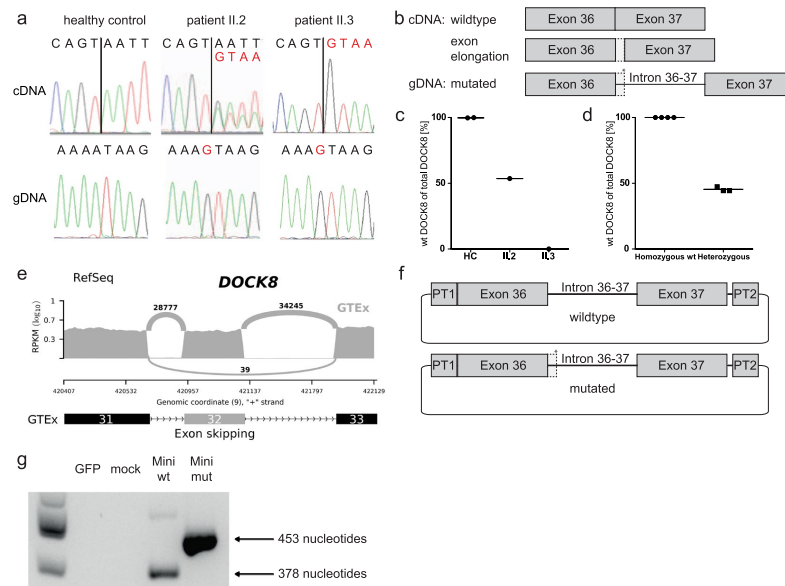


Figure 3. Genetic analysis of *DOCK8*. (a) T cell blast cDNA chromatograms show wildtype sequence in a healthy control, double peaks in patient II.2 and altered sequence in patient II.3. Both patients' gDNA is homozygous for alteration c.4626 + 76 A > G; vertical black lines: 3' junction of exon 36; black letters: wildtype; red letters: altered sequence. (b) Schematic model of affected region in *DOCK8* gDNA and transcripts showing exon extension (dotted line) due to the novel splice site (*) introduced at c.4626 + 76 A > G; filled boxes: exons; horizontal line: intronic region. (c) Quantification of wildtype and altered transcripts in T cell blasts by ddPCR indicating percentages of wildtype (wt) of total *DOCK8* transcripts in patient II.2, patient II.3 and healthy controls (HC). (d) ddPCR analysis of healthy controls (homozygous wt) and healthy carriers of a c.3120 + 1 G > T *DOCK8* alteration resulting in exon 25 skipping (heterozygous). (e) Sashimi plot of RNA sequencing data based on GTEx samples^{21,22} showing exon 32 skipping as a rare event; read counts accumulated over all samples. (f) Schematic model of wildtype and mutated minigene vectors. Sequence tags (PT1/PT2) flanked the minigene sequence to differentiate minigene transcripts from endogenous *DOCK8* transcripts; filled boxes: exons; dotted line: exon extension; horizontal line: intronic regions; *: novel splice site. (g) The altered or physiologic transcription products of the minigene vectors were differentiated by size. Agarose gel with canonical splice site usage (378 nucleotide transcript) in cDNA of control PBMCs transfected with wildtype (Mini wt) and usage of the novel splice site (453 nucleotide transcript) in cDNA of PBMCs transfected with the mutated minigene vector (Mini mut); GFP- and mock-transfected as negative controls.

With this inconclusive WGS analyses and the clinical presentation of patient II.2 partly suggesting *DOCK8*-HIES, we reassessed *DOCK8* by Sanger sequencing. Sequencing *DOCK8* cDNA of patient II.2's T cell blasts revealed double peaks downstream of exon 36 (Fig. 3a). We identified these double peaks as result of a combination of physiologic *DOCK8* transcripts and transcripts with exon 36 extended by 75 nucleotides at the 3' end resulting in a premature stop codon after 18 nucleotides (Fig. 3a,b). We consulted the GTEx dataset^{21,22} for alternatively spliced *DOCK8* transcripts with extension of exon 36 and found rare events of exon extension by 16 or 133 nucleotides as visualized by Sashimi plot and the corresponding percent spliced in (psi) analysis (Supplementary Fig. S3). Although these rare events of extended exons suggest susceptibility of the intron downstream of exon 36 to splicing, an alternatively spliced *DOCK8* transcript with extension of exon 36 by 75 nucleotides was not present in the dataset. gDNA sequencing of the introns flanking exon 36 of patient II.2 and re-analyzing the WGS data identified a homozygous intronic nucleotide exchange (c.4626 + 76 A > G) introducing a novel splice site in *DOCK8* (Fig. 3a).

Both parents and the healthy sister were heterozygous for the c.4626 + 76 A > G variant which has not been reported in the databases dbSNP²³ and gnomAD²⁴. Droplet digital PCR (ddPCR) confirmed the cDNA sequencing results of patient II.2 (Fig. 3c) showing almost equal parts of wildtype *DOCK8* transcripts and altered elongated transcripts. To evaluate if expression of about 50% wildtype *DOCK8* transcript is sufficient to prevent a *DOCK8*-HIES phenotype, we performed ddPCR analyses with *DOCK8* cDNA of T cell blasts of healthy carriers of a heterozygous *DOCK8* c.3120 + 1 G > T mutation resulting in skipping of exon 25. All three healthy carriers

had equal amounts of wildtype and truncated *DOCK8* transcripts suggesting that the *DOCK8* gene is haploinsufficient (Fig. 3d).

In patient II.3 the homozygous intronic *DOCK8* alteration (c.4626 + 76 A > G) as in patient II.2 was identified soon after birth (Fig. 3a). In contrast to patient II.2, in patient II.3 all *DOCK8* transcripts showed the alteration with extension of exon 36 (Fig. 3a,c). Additionally, exon 32 was missing in about half of patient II.3's *DOCK8* transcripts. gDNA sequencing of both flanking introns of exon 32 revealed no genetic alteration in patient II.3. Due to haploinsufficiency of *DOCK8* we concluded that exon 32 skipping was not the cause of disease in patient II.3. This was supported by the fact that exon 32 skipping was also found as a rare event in the GTEx dataset^{21,22} as visualized by Sashimi plot and the corresponding psi analysis (Fig. 3e, Supplementary Fig. S3).

Since the intronic variant c.4626 + 76 A > G results in a novel donor splice site (AT > GT) in the intron between exon 36 and 37 of *DOCK8* and as *DOCK8* transcripts were differently affected in the two patients we assessed splice site usage by *in silico* analyses. Splice site prediction tools calculated higher scores for the novel donor splice site compared to the canonical splice site (NNSPLICE0.9²⁵ score: 0.97 and 0.86; HSF²⁶ score: 86.53 and 80.99; SplicePort²⁷ score: 0.58 and 0.14 of novel splice site and canonical splice site, respectively). Moreover, SpliceAid2²⁸ predicted the loss of multiple binding sites for splicing factors as a result of the c.4626 + 76 A > G alteration indicating a reduction of splicing activity at the canonical splice site. Thus, these bioinformatics analyses indicated the variant as a stronger donor site that outperforms the canonical donor site leading to altered transcripts. To verify the *in silico* prediction *in vitro* we introduced a minigene vector containing the intronic variant c.4626 + 76 A > G or the wildtype sequence into PBMCs of healthy individuals (Fig. 3f). In presence of the novel splice site, we solely detected altered transcripts with exon extension in PBMCs of healthy controls (Fig. 3g). Thus, the minigene analysis supported the exclusive expression of altered transcripts with an extended exon 36 as observed in patient II.3.

DOCK8 expression analyses. The c.4626 + 76 A > G alteration found in patients II.2 and II.3 leads to a premature stop codon in the *DOCK8* protein and consequently a lack of *DOCK8* protein as observed in western blot and flow cytometric analyses in PBMCs of patient II.3 (Fig. 4). Western blot analysis of PBMCs of patient II.2, however, showed expression of *DOCK8* protein (Fig. 4a, Supplementary Fig. S4). Detailed lymphocyte subset analysis revealed no *DOCK8* protein expression in B cells of patient II.2, whereas most NK cells expressed *DOCK8* (Fig. 4b). The majority of CD4⁺ and CD8⁺ T cells expressed *DOCK8*, while about 20–30% were *DOCK8* negative. Naïve T cells and the majority of T_{EMRA} cells did not express *DOCK8*, whereas most effector memory T cells did express *DOCK8* protein (Fig. 4c). The presence of *DOCK8* protein in cell subsets corresponded with the transcript analysis of sorted lymphocyte subsets of patient II.2: B cells had only altered transcripts with exon extension in accordance with a missing expression of *DOCK8* protein (Fig. 4d); NK and T cells expressed wildtype and altered *DOCK8* transcripts.

To explain the expression of wildtype *DOCK8* transcript and *DOCK8* protein in NK and T cells of patient II.2, we performed gDNA sequencing of sorted cells. Cells of patient II.2 were subdivided first by their *DOCK8* expression and subsequently by different lymphocyte subsets (Fig. 5a). B cells (*DOCK8*⁻CD19⁺) and *DOCK8*⁻negative non-B cells (*DOCK8*⁻CD19⁻) were homozygous for the novel splice site (Fig. 5b). *DOCK8*-expressing cells were divided into T cells (*DOCK8*⁺CD19⁻CD3⁺) and NK cells (*DOCK8*⁺CD19⁻CD56⁺). A double peak for the mutated and the wildtype sequence was detected in *DOCK8*-expressing NK cells; hence, likely explaining *DOCK8* protein expression in the majority of NK cells by somatic gDNA reversion to wildtype sequence. *DOCK8*-positive T cells showed in addition to the novel splice site small double peaks at position c.4626 + 76, c.4626 + 77, and c.4626 + 80.

Further sorting of T cell subsets explained *DOCK8* protein re-expression in CD4⁺ T cells by somatic alterations at position c.4626 + 76 and c.4626 + 77 reverting the sequence to wildtype or destroying the novel splice site (Fig. 5c). In the presence of the somatic variant c.4626 + 80 G > C splice site prediction tools calculated lower scores for the novel splice site (NNSPLICE0.9²⁵ score: 0.97 and 0.10; HSF²⁶ score: 86.53 and 74.52; SplicePort²⁷ score: 0.58 and -0.56 of novel splice site without and in the presence of the variant c.4626 + 80 G > C). Hence, *DOCK8* expression in CD8⁺ T cells resulted from reuse of the physiologic splice site due to weakening of the novel splice site by the somatic variant c.4626 + 80 G > C. Moreover, SpliceAid2²⁸ predicted a novel binding site of the splicing activator DAZAP1²⁹ as a result of the c.4626 + 80 G > C alteration indicating an increase of splicing activity at the canonical splice site.

Discussion

Our experience of two siblings with HIES findings shows the complex process of a molecular genetic diagnosis including verification of the identified homozygous intronic *DOCK8* variant c.4626 + 76 A > G as disease-causing in the presence of somatic alterations. Hyperextensible joints and impaired Y705-STAT3 phosphorylation pointed towards STAT3-HIES in patient II.2^{1,2,5,6}. But in contrast to STAT3-HIES patients, who present with a reduction of Th17 cell counts due to diminished STAT3 function^{8,9}, the patient II.2 presented with normal Th17 cell counts. To explain her normal Th17 cell counts despite a STAT3 phosphorylation defect, we revealed intact IL21-induced STAT3 activation in patient II.2's lymphocytes as an alternative route for Th17 differentiation^{30,31}. Her recurrent viral infections, high eosinophil counts, multiple food allergies, and failure to thrive raised suspicion of *DOCK8*-HIES^{3-5,11}, while the lack of lymphopenia, rather normal to high lymphocyte counts, and particularly the *DOCK8* protein expression in PBMCs argued against *DOCK8*-HIES. However, assessment of *DOCK8* transcripts and subsequent gDNA sequencing of intronic regions by Sanger technique identified the homozygous intronic *DOCK8* variant c.4626 + 76 A > G, creating a novel splice site, retrospectively also found in the NGS data. During the time of identifying this variant, the second affected child (patient II.3) was born carrying the same homozygous *DOCK8* alteration yet missing *DOCK8* protein expression in her PBMCs. *In silico* and *in vitro* analyses showed that the novel splice site was preferentially used by the spliceosome regardless of the presence

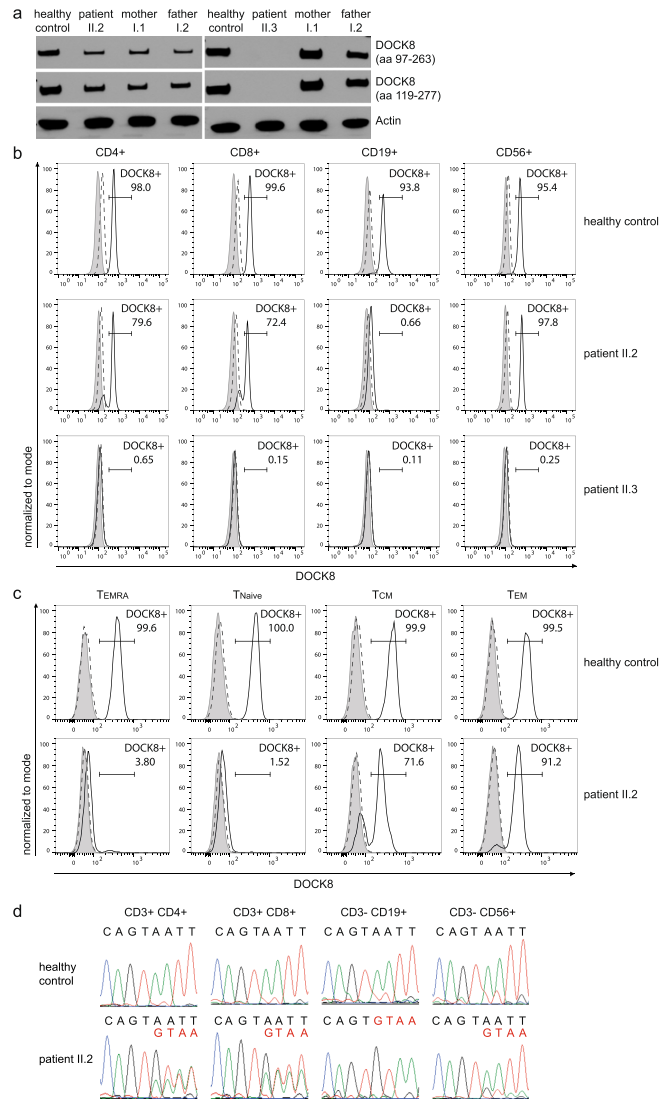


Figure 4. DOCK8 expression analysis. **(a)** Western blot analysis of whole PBMC lysates shows DOCK8 expression in patient II.2 and not in patient II.3 with two different DOCK8 antibodies (immunogen indicated in brackets; aa: amino acid); Actin as a loading control. Full-length western blots are provided in the Supplementary Appendix (Supplementary Fig. S4). **(b)** Flow cytometry of patient II.2 showed DOCK8 expression in majority of NK cells and T cells but no DOCK8 expression in B cells. All cell subsets of patient II.3 lack DOCK8 expression. Gray area: unstained; dashed line: isotype control; solid line: DOCK8 staining. **(c)** T cell subsets defined by naive T cells (CCR7⁺CD45RA⁺), central memory T cells (CCR7⁺CD45RA⁻), effector memory T cells (CCR7⁻CD45RA⁺) and T_{EMRA} cells (CCR7⁻CD45RA⁺) showed no DOCK8 expression in T_{EMRA} and naive T cells and DOCK8 expression in majority of central and effector memory T cells of patient II.2 compared to DOCK8 expression in all T cell subsets of a healthy control. **(d)** Sequencing of cDNA reveals double peaks in chromatograms of T and NK cells of patient II.2 indicating wildtype (black letters) and altered (red letters) transcripts. cDNA chromatogram of B cells shows only single peaks indicating altered transcripts.

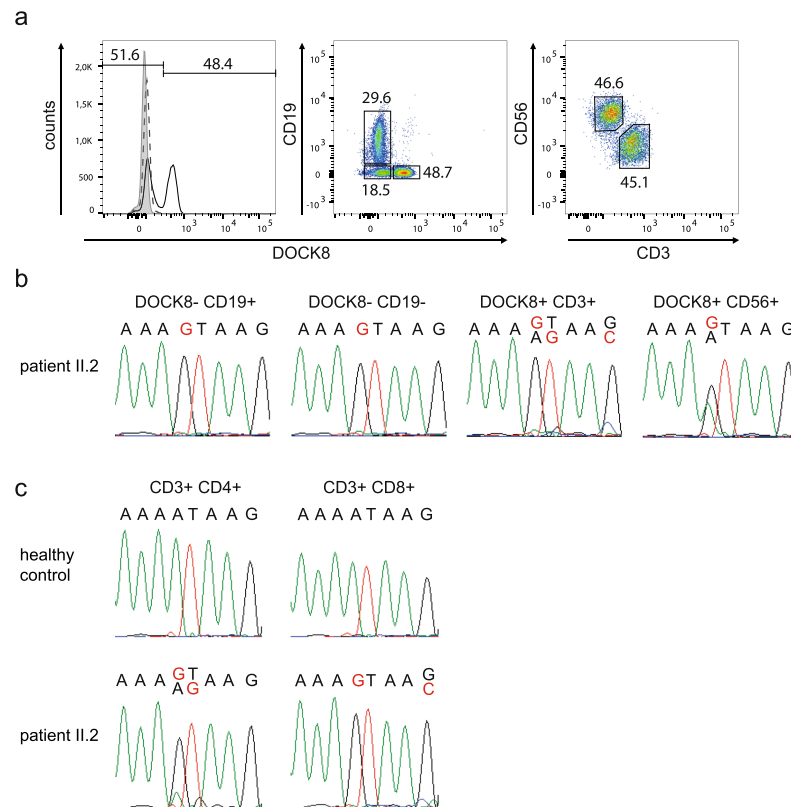


Figure 5. Analysis of somatic alterations in *DOCK8*. **(a)** Gating strategy to sort lymphocyte subsets according to their *DOCK8* expression. PBMCs of patient II.2 were gated for lymphocytes and then *DOCK8*-negative cells into B cells (*DOCK8*⁺*CD19*⁺) and non-B cells (*DOCK8*⁺*CD19*⁻), and *DOCK8*-positive cells into T cells (*DOCK8*⁺*CD19*⁻*CD3*⁺) and NK cells (*DOCK8*⁺*CD19*⁻*CD56*⁺). **(b)** gDNA sequence of sorted cells of patient II.2 had a homozygous peak for the c.4626 + 76 A > G alteration (red letter) in T and B cells and a double peak with altered (red letter) and wildtype (black letter) sequence in NK cells. **(c)** gDNA sequence of unfixed and unpermeabilized PBMCs of patient II.2 sorted according to the lymphocyte subsets CD4⁺ and CD8⁺ T cells showing double peaks with altered (red letter) and wildtype (black letter) sequence in CD4⁺ T cells at positions c.4626 + 76 and c.4626 + 77 and at position c.4626 + 80 in CD8⁺ T cells.

of the canonical splice site, confirming the variant c.4626 + 76 A > G as disease-causing. Hence, the exclusive use of the novel splice site explained the lack of *DOCK8* protein in PBMCs of patient II.3 and B cells of patient II.2.

Yet why was *DOCK8* protein expressed in NK cells and parts of T cells of patient II.2? Since somatic reversions have been reported in *DOCK8*-HIES^{32–34}, we investigated *DOCK8* transcripts in NK cells and T cell subsets confirming our hypothesis of somatic alterations. Consequently, most of patient II.2's T cells were able to produce wildtype *DOCK8* transcripts likely leading to a survival advantage and clonal expansion of *DOCK8* expressing T cells under selective pressure, e.g. exerted by viral infections, as reported for *DOCK8*-HIES and other PIDs^{32,34,35}.

This selective advantage of *DOCK8* expressing T cells may also explain why we did not observe a more pronounced shift from memory CD8⁺ T cells to T_{EMRA} cells in patient II.2, as reported to be characteristic of *DOCK8*-HIES patients due to reduced memory cell persistence³⁶. We suggest that the *DOCK8* expression, observed in the majority of her CD8⁺ effector memory T cells, rescued memory cell persistence and resulted in a reduced shift towards a T_{EMRA} phenotype. The dependence of memory T cell persistence on *DOCK8* expression was further supported by the fact that the majority of her T_{EMRA} cells were *DOCK8* negative. The skewed T cell distribution of more than 80% effector memory and T_{EMRA} cells of total T cells likely also explains the impaired IL6-induced STAT3 activation in lymphocytes of patient II.2. Only naïve T cells and a few central memory T cells are reported to show STAT3 phosphorylation after IL6 stimulation, whereas in effector memory T cells and

T_{EMRA} cells STAT3 is not activated by IL6 stimulation^{37–39}. Furthermore, IL6 does not phosphorylate STAT3 in B and NK cells, whereas IL10 induces STAT3 phosphorylation in all lymphocyte subsets⁴⁰. Hence, once T cell subpopulations, including naïve T cells, normalized in patient IL.2 after HSCT, IL6-induced STAT3 phosphorylation also normalized and was therefore not caused by the *DOCK8* alteration but secondarily caused due to shifted T cell subsets.

Taken together, HSCT cured patient IL.3, who was diagnosed early, while patient IL.2 still requires intensive treatment underscoring the need for and the benefit of an early diagnosis. The fact that the autosomal recessive WGS analysis did not prioritize the disease-causing alteration and that within the GTEx dataset^{21,22} we found evidence that *DOCK8* exon 36 is susceptible to alternative splicing demonstrates, that integrating existing RNA sequencing data into WES and WGS analyses may help to prioritize variants in introns susceptible to alternative splicing⁴¹. To date, transcriptomics is often used as a complementary diagnostic tool if patients remain without molecular diagnosis after WES or WGS^{41,42}. However, molecular diagnosis might have been delayed even with additional transcriptome analysis as patient IL.2 expressed altered and due to somatic alterations wildtype *DOCK8* transcripts.

In conclusion, the complex diagnostic process of these patients shows how somatic alterations compromise molecular diagnostics and reminds to keep the clinical presentation in mind calling for a close interaction between clinicians, scientists, and bioinformaticians.

Material and Methods

Patients, their healthy parents, molecularly defined *DOCK8*-HIES patients, healthy *DOCK8*-HIES carriers, and healthy controls were included in this study after written informed consent given by patients or their legal guardians. Patients' clinical, immunologic, and molecular findings were assessed by Next Generation Sequencing (NGS), expression and splicing analysis, and cell phenotyping and compared to controls as indicated; for detailed methods see Supplementary Materials and Methods. The study was approved by the local reviewing board (Ethikkommission bei der Medizinischen Fakultät der Ludwig-Maximilians-Universität München, #381-13), written informed consent was obtained. All research was performed in accordance with relevant guidelines and regulations.

Data Availability Statement

The datasets generated and analyzed during this study are not publicly available due to country specific restrictions on data safety protecting the privacy of the involved study participants.

References

- Holland, S. M. *et al.* STAT3 mutations in the hyper-IgE syndrome. *N Engl J Med* **357**, 1608–1619, <https://doi.org/10.1056/NEJMoa073687> (2007).
- Minegishi, Y. *et al.* Dominant-negative mutations in the DNA-binding domain of STAT3 cause hyper-IgE syndrome. *Nature* **448**, 1058–1062, <https://doi.org/10.1038/nature06096> (2007).
- Engelhardt, K. R. *et al.* Large deletions and point mutations involving the dedicator of cytokinesis 8 (*DOCK8*) in the autosomal-recessive form of hyper-IgE syndrome. *J Allergy Clin Immunol* **124**, 1289–1302 e1284, <https://doi.org/10.1016/j.jaci.2009.10.038> (2009).
- Zhang, Q. *et al.* Combined immunodeficiency associated with *DOCK8* mutations. *N Engl J Med* **361**, 2046–2055, <https://doi.org/10.1056/NEJMoa0905506> (2009).
- Hagl, B. *et al.* Key findings to expedite the diagnosis of hyper-IgE syndromes in infants and young children. *Pediatr Allergy Immunol* **27**, 177–184, <https://doi.org/10.1111/pai.12512> (2016).
- Boos, A. C. *et al.* Atopic dermatitis, STAT3- and *DOCK8*-hyper-IgE syndromes differ in IgE-based sensitization pattern. *Allergy* **69**, 943–953, <https://doi.org/10.1111/all.12416> (2014).
- Sowerwine, K. J., Holland, S. M. & Freeman, A. F. Hyper-IgE syndrome update. *Ann N Y Acad Sci* **1250**, 25–32, <https://doi.org/10.1111/j.1749-6632.2011.06387.x> (2012).
- Milner, J. D. *et al.* Impaired T(H)17 cell differentiation in subjects with autosomal dominant hyper-IgE syndrome. *Nature* **452**, 773–776, <https://doi.org/10.1038/nature06764> (2008).
- Renner, E. D. *et al.* Novel signal transducer and activator of transcription 3 (STAT3) mutations, reduced T(H)17 cell numbers, and variably defective STAT3 phosphorylation in hyper-IgE syndrome. *J Allergy Clin Immunol* **122**, 181–187, <https://doi.org/10.1016/j.jaci.2008.04.037> (2008).
- Pai, S. Y. *et al.* Flow cytometry diagnosis of dedicator of cytokinesis 8 (*DOCK8*) deficiency. *J Allergy Clin Immunol* **134**, 221–223, <https://doi.org/10.1016/j.jaci.2014.02.023> (2014).
- Aydin, S. E. *et al.* *DOCK8* deficiency: clinical and immunological phenotype and treatment options - a review of 136 patients. *J Clin Immunol* **35**, 189–198, <https://doi.org/10.1007/s10875-014-0126-0> (2015).
- Engelhardt, K. R. *et al.* The extended clinical phenotype of 64 patients with dedicator of cytokinesis 8 deficiency. *J Allergy Clin Immunol* **136**, 402–412, <https://doi.org/10.1016/j.jaci.2014.12.1945> (2015).
- Uygun, D. F. K. *et al.* Hematopoietic stem cell transplantation from unrelated donors in children with *DOCK8* deficiency. *Pediatr Transplant*. <https://doi.org/10.1111/petr.13015> (2017).
- Nijman, I. J. *et al.* Targeted next-generation sequencing: a novel diagnostic tool for primary immunodeficiencies. *J Allergy Clin Immunol* **133**, 529–534, <https://doi.org/10.1016/j.jaci.2013.08.032> (2014).
- Gallo, V. *et al.* Diagnostics of Primary Immunodeficiencies through Next-Generation Sequencing. *Front Immunol* **7**, 466, <https://doi.org/10.3389/fimmu.2016.00466> (2016).
- Picard, C. *et al.* International Union of Immunological Societies: 2017 Primary Immunodeficiency Diseases Committee Report on Inborn Errors of Immunity. *J Clin Immunol* **38**, 96–128, <https://doi.org/10.1007/s10875-017-0464-9> (2018).
- Grimbacher, B. *et al.* Genetic linkage of hyper-IgE syndrome to chromosome 4. *Am J Hum Genet* **65**, 735–744, <https://doi.org/10.1086/302547> (1999).
- Okabe, T. *et al.* RICS, a novel GTPase-activating protein for Cdc42 and Rac1, is involved in the beta-catenin-N-cadherin and N-methyl-D-aspartate receptor signaling. *J Biol Chem* **278**, 9920–9927, <https://doi.org/10.1074/jbc.M208872003> (2003).
- Kawashima, T. *et al.* A Rac GTPase-activating protein, MgcRacGAP, is a nuclear localizing signal-containing nuclear chaperone in the activation of STAT transcription factors. *Mol Cell Biol* **29**, 1796–1813, <https://doi.org/10.1128/MCB.01423-08> (2009).
- Tonozuka, Y. *et al.* A GTPase-activating protein binds STAT3 and is required for IL-6-induced STAT3 activation and for differentiation of a leukemic cell line. *Blood* **104**, 3550–3557, <https://doi.org/10.1182/blood-2004-03-1066> (2004).
- Consortium, G. T. The Genotype-Tissue Expression (GTEx) project. *Nat Genet* **45**, 580–585, <https://doi.org/10.1038/ng.2653> (2013).
- Consortium, G. T. Human genomics. The Genotype-Tissue Expression (GTEx) pilot analysis: multitissue gene regulation in humans. *Science* **348**, 648–660, <https://doi.org/10.1126/science.1262110> (2015).

23. Sherry, S. T. *et al.* dbSNP: the NCBI database of genetic variation. *Nucleic Acids Res* **29**, 308–311 (2001).
24. Lek, M. *et al.* Analysis of protein-coding genetic variation in 60,706 humans. *Nature* **536**, 285–291, <https://doi.org/10.1038/nature19057> (2016).
25. Reese, M. G., Eeckman, F. H., Kulp, D. & Haussler, D. Improved splice site detection in Genie. *J Comput Biol* **4**, 311–323, <https://doi.org/10.1089/cmb.1997.4.311> (1997).
26. Desmet, F. O. *et al.* Human Splicing Finder: an online bioinformatics tool to predict splicing signals. *Nucleic Acids Res* **37**, e67, <https://doi.org/10.1093/nar/gkp215> (2009).
27. Dogan, R. I., Getoor, L., Wilbur, W. J. & Mount, S. M. SplicePort—an interactive splice-site analysis tool. *Nucleic Acids Res* **35**, W285–291, <https://doi.org/10.1093/nar/gkm407> (2007).
28. Piva, F., Giulietti, M., Burini, A. B. & Principato, G. SpliceAid 2: a database of human splicing factors expression data and RNA target motifs. *Hum Mutat* **33**, 81–85, <https://doi.org/10.1002/humu.21609> (2012).
29. Choudhury, R. *et al.* The splicing activator DAZAP1 integrates splicing control into MEK/Erk-regulated cell proliferation and migration. *Nat Commun* **5**, 3078, <https://doi.org/10.1038/ncomms4078> (2014).
30. Korn, T. *et al.* IL-21 initiates an alternative pathway to induce proinflammatory T(H)17 cells. *Nature* **448**, 484–487, <https://doi.org/10.1038/nature05970> (2007).
31. Schwerdt, T. *et al.* A biallelic mutation in IL6ST encoding the GPI30 co-receptor causes immunodeficiency and craniosynostosis. *J Exp Med* **214**, 2547–2562, <https://doi.org/10.1084/jem.20161810> (2017).
32. Jing, H. *et al.* Somatic reversion in dedicator of cytokinesis 8 immunodeficiency modulates disease phenotype. *J Allergy Clin Immunol* **133**, 1667–1675, <https://doi.org/10.1016/j.jaci.2014.03.025> (2014).
33. Kienzler, A. K. *et al.* Hypomorphic function and somatic reversion of DOCK8 cause combined immunodeficiency without hyper-IgE. *Clin Immunol* **163**, 17–21, <https://doi.org/10.1016/j.clim.2015.12.003> (2016).
34. Wada, T. & Candotti, F. Somatic mosaicism in primary immune deficiencies. *Curr Opin Allergy Clin Immunol* **8**, 510–514, <https://doi.org/10.1097/ACI.0b013e328314b651> (2008).
35. Palendira, U. *et al.* Expansion of somatically reverted memory CD8+ T cells in patients with X-linked lymphoproliferative disease caused by selective pressure from Epstein-Barr virus. *J Exp Med* **209**, 913–924, <https://doi.org/10.1084/jem.20112391> (2012).
36. Randall, K. L. *et al.* DOCK8 deficiency impairs CD8 T cell survival and function in humans and mice. *The Journal of experimental medicine* **208**, 2305–2320, <https://doi.org/10.1084/jem.20110345> (2011).
37. Willinger, T., Freeman, T., Hasegawa, H., McMichael, A. J. & Callan, M. F. Molecular signatures distinguish human central memory from effector memory CD8 T cell subsets. *J Immunol* **175**, 5895–5903 (2005).
38. Yang, R. *et al.* IL-6 promotes the differentiation of a subset of naive CD8+ T cells into IL-21-producing B helper CD8+ T cells. *J Exp Med* **213**, 2281–2291, <https://doi.org/10.1084/jem.20160417> (2016).
39. Jones, G. W. *et al.* Loss of CD4+ T cell IL-6R expression during inflammation underlines a role for IL-6 trans signaling in the local maintenance of Th17 cells. *J Immunol* **184**, 2130–2139, <https://doi.org/10.4049/jimmunol.0901528> (2010).
40. Davies, R., Vogelsang, P., Jonsson, R. & Appel, S. An optimized multiplex flow cytometry protocol for the analysis of intracellular signaling in peripheral blood mononuclear cells. *J Immunol Methods* **436**, 58–63, <https://doi.org/10.1016/j.jim.2016.06.007> (2016).
41. Kremer, L. S. *et al.* Genetic diagnosis of Mendelian disorders via RNA sequencing. *Nat Commun* **8**, 15824, <https://doi.org/10.1038/ncomms15824> (2017).
42. Cummings, B. B. *et al.* Improving genetic diagnosis in Mendelian disease with transcriptome sequencing. *Sci Transl Med* **9**, <https://doi.org/10.1126/scitranslmed.aal5209> (2017).

Acknowledgements

We thank all patients and their families for their participation, the primary care physicians, technicians and nurses for their support as well as technical assistance, the Hartwig Medical Foundation for the WGS, Stephen Starck for critical language reviewing and Talal Chatila, Lucie Grodecká, Almut Meyer-Bahlburg and Michael Sattler for scientific discussions. This work was supported by the Wilhelm-Sander foundation (2013.015.2), the German Research Foundation (DFG RE2799/6-1), the Fritz-Bender foundation (all to E.D.R.), the EU Horizon2020 Collaborative Research Project SOUND (633974) (to J.G.), and the Spanish Ministry of Economy and Competitiveness, Centro de Excelencia Severo Ochoa, and to the EMBL partnership and of the CERCA Programme/Generalitat de Catalunya. Data included in this publication are part of a medical thesis at the School of Medicine, LMU Munich (B.D.S.).

Author Contributions


B.H., B.D.S., S.T., S.B., A.C.E., A.P., D.S., performed research and analyzed data; C.M., C.W., I.J.N., S.V., J.R., T.M., J.G., J.S.O., M.E.v.G. analyzed data; B.H., B.D.S., E.D.R. analyzed clinical data; B.H., B.D.S. performed STAT3 analysis and post-sort gDNA sequencing; B.H. performed cDNA analysis, minigene analysis and isolated fibroblasts, B.D.S. performed T subpopulation, DOCK8 protein expression and autoantibody analysis; B.H., B.D.S., E.D.R. designed the research and were the principal writers of the manuscript. All of the authors reviewed the manuscript and contributed in writing.

Additional Information

Supplementary information accompanies this paper at <https://doi.org/10.1038/s41598-018-34953-z>.

Competing Interests: The authors declare no competing interests.

Publisher's note: Springer Nature remains neutral with regard to jurisdictional claims in published maps and institutional affiliations.

 **Open Access** This article is licensed under a Creative Commons Attribution 4.0 International License, which permits use, sharing, adaptation, distribution and reproduction in any medium or format, as long as you give appropriate credit to the original author(s) and the source, provide a link to the Creative Commons license, and indicate if changes were made. The images or other third party material in this article are included in the article's Creative Commons license, unless indicated otherwise in a credit line to the material. If material is not included in the article's Creative Commons license and your intended use is not permitted by statutory regulation or exceeds the permitted use, you will need to obtain permission directly from the copyright holder. To view a copy of this license, visit <http://creativecommons.org/licenses/by/4.0/>.

© The Author(s) 2018

Somatic alterations compromised molecular diagnosis of DOCK8 hyper-IgE syndrome caused by a novel intronic splice site mutation

Beate Hagl PhD^{1,2}, Benedikt D Spielberger MD^{1,2}, Silvia Thoene PhD^{3,4,5}, Sophie Bonnal PhD^{6,7}, Christian Mertes MSc⁸, Christof Winter MD, PhD^{3,4,5}, Isaac J Nijman PhD⁹, Shira Verduin MSc⁹, Andreas C Eberherr MSc¹, Anne Puel PhD^{10,11,12}, Detlev Schindler MD¹³, Jürgen Ruland MD^{3,4,5,14}, Thomas Meitinger MD, PhD¹⁵, Julien Gagneur PhD^{8,16}, Jordan S Orange MD, PhD^{17,18,19}, Marielle E van Gijn PhD⁹, Ellen D Renner MD^{1,2,20,*}

¹Chair and Institute of Environmental Medicine, UNIKA-T, Technical University of Munich and Helmholtz Zentrum Munich, Munich/Augsburg, Germany; ²University Children's Hospital, Dr. von Haunersches Kinderspital, Ludwig Maximilian University, Munich, Germany; ³Institute of Clinical Chemistry and Pathobiochemistry, Klinikum rechts der Isar, Technical University of Munich, Munich, Germany; ⁴German Cancer Consortium (DKTK), partner site Munich, Munich, Germany; ⁵German Cancer Research Center (DKFZ), Heidelberg, Germany; ⁶Centre for Genomic Regulation (CRG), The Barcelona Institute of Science and Technology, Dr. Aiguader 88, Barcelona 08002, Spain; ⁷Universitat Pompeu Fabra (UPF), Barcelona, Spain; ⁸Department of Informatics, Technical University of Munich, Garching, Germany; ⁹Department of Genetics, University Medical Center Utrecht, Utrecht, The Netherlands; ¹⁰Laboratory of Human Genetics of Infectious Diseases, Necker Branch, Necker Medical School, Paris, France; ¹¹Paris Descartes University, Sorbonne Paris Cité, Institut Imagine, Paris, France; ¹²St Giles Laboratory of Human Genetics of Infectious Diseases, Rockefeller Branch, Rockefeller University, New York, NY, USA; ¹³Department of Human Genetics, University of Würzburg, Würzburg, Germany; ¹⁴German Center for Infection Research (DZIF), partner site Munich, Munich, Germany; ¹⁵Institute of Human Genetics, Technical University of Munich and Helmholtz Zentrum Munich, Neuherberg, Germany; ¹⁶Quantitative Biosciences Munich, Gene Center, Department of Biochemistry, Ludwig Maximilian University, Munich, Germany; ¹⁷Center for Human Immunobiology of Texas Children's Hospital/Department of Pediatrics, Baylor College of Medicine, Houston, TX, USA; ¹⁸Department of Pediatrics, Division of Immunology, Allergy, and Rheumatology, Baylor College of Medicine, and Texas Children's Hospital, Houston, TX, USA; ¹⁹Department of Pediatrics, Baylor College of Medicine, and Texas Children's Hospital, Houston, TX, USA; ²⁰Hochgebirgsklinik and Christine-Kühne-Center for Allergy Research and Education (CK-Care), Davos, Switzerland

B.H. and B.D.S. contributed equally to this work

SUPPLEMENTARY APPENDIX

TABLE OF CONTENTS:

Supplementary Material and Methods	3
Patients, clinical and immunologic work-up	3
Genetic analyses	3
DOCK8 mRNA expression analyses	4
DOCK8 protein assessment	4
DOCK8 splicing analyses	5
Supplementary Figures	6
Supplementary Figure S1: Autoantibody analysis	6
Supplementary Figure S2: ARHGAP32 analysis	7
Supplementary Figure S3: <i>In silico</i> analysis of preexisting RNA sequencing data	8
Supplementary Figure S4: DOCK8 western blot analysis	10
References	12

Supplementary Material and Methods:

Patients, clinical and immunologic work-up

A consanguineous family of Turkish descent with two children with HIES findings and a healthy sibling was assessed. The study was approved by the local reviewing board (Ethikkommission bei der Medizinischen Fakultät der Ludwig-Maximilians-Universität München, #381-13), written informed consent of patients or their legal guardians was obtained. All research was performed in accordance with relevant guidelines and regulations.

Differential blood count and serum immunoglobulin level were assessed as to standardized protocols. We isolated peripheral blood mononuclear cells (PBMCs) from venous blood using Biocoll Separating Solution (BIOCHROM AG, Berlin, Germany). Lymphocyte stimulation with an antigen mixture and different mitogens was performed as previously described¹.

Lymphocyte subsets were defined by total T cells (CD3⁺), T helper cells (CD3⁺CD4⁺), cytotoxic T cells (CD3⁺CD8⁺), Th17 cells (CD3⁺CD4⁺IL17⁺IFN γ ⁺), total B cells (CD19⁺), memory B cells (CD19⁺CD27⁺), and NK cells (CD16⁺CD56⁺), stained with the according antibodies, and analyzed by flow cytometry (BD FACSCalibur and BD LSRFortessa, BD Biosciences, San Jose, CA, USA) as previously described.¹ Subdivided T cell subsets were defined by naïve T cells (CD3⁺CCR7⁺CD45RA⁻), central memory T cells (CD3⁺CCR7⁺CD45RA⁺), effector memory T cells (CD3⁺CCR7⁻CD45RA⁺) and T_{EMRA} cells (CD3⁺CCR7⁻CD45RA⁺) and stained according to the following protocol adapted from ². Briefly, cells were treated with Biolegend Aqua Zombie dye BV510 to exclude dead cells according to the manufacturer's instruction. After staining with anti-CCR7 BV421, anti-CD3 APC-H7, anti-CD4 BV711, anti-CD8 PE, anti-CD19 PE-Cy7, anti-CD56 APC, anti-CD45RA BV650 (all BD) cells were analyzed by flow cytometry. Patients' values were compared to age-matched references as previously described¹ or to healthy individuals.

STAT3 tyrosine phosphorylation was assessed in PBMCs by flow cytometry using the BD Phosflow reagents per the manufacturer's instruction (BD Biosciences) and by western blot using antibodies to Phospho-STAT3 (Tyr705), STAT3 and beta-Actin (all Cell Signaling, Danvers, MA, USA) as previously described.³ To analyze a putative effect of autoantibodies on STAT3 phosphorylation, PBMCs of a healthy control were incubated overnight in the absence or presence of 10% patient or different control sera (adopted from ⁴) and Phospho-STAT3 (Tyr 705) was measured by flow cytometry after IL6 and IL10 stimulation. The effect of ARHGAP32 on STAT3 phosphorylation was assessed by transfecting a wildtype *ARHGAP32* vector (OriGene, Rockville, MD, USA) into healthy control PBMCs by nucleofection using the Human T Cell Nucleofector Kit and a Nucleofector 2b (both Lonza, Basel, Switzerland) followed by flow cytometric analysis as well as by assessing STAT3 phosphorylation in HAP1 *ARHGAP32* knock-out cells and wildtype HAP1 cells (Horizon, Cambridge, UK) by western blot.

Genetic analyses

Targeted next-generation sequencing was performed as previously described⁵. Sample prep (TruSeq DNA, input 250 ng) and the Illumina's HiSeqX sequencing platform were used according to manufacturer's instructions to perform WGS. Illumina data were processed with the inhouse developed pipeline v1.2.1 (<https://github.com/UMCUGenetics/IAP>) including GATK v3.2.2⁶ according to the best practice guidelines.^{7,8} Briefly, paired end reads were mapped with BWA-MEM v0.7.5a⁹ to GRCh37, duplicates marked, lanes merged, and indels realigned. Base Quality Score recalibration was left out since it did not improve our results significantly. Next, GATK Haplotypecaller was used to call SNPs and indels to create GVCFs. These GVCFs were genotyped with GATK's GenotypeGVCFs for the described family. Variants were flagged as PASS if none of the following criteria was fulfilled: QD<2.0,

3

MQ<40.0, FS>60.0, HaplotypeScore>13.0, MQRankSum<-12.5, ReadPosRankSum<-8.0, snpclusters>=3 in 35bp. For indels: QD<2.0, FS>200.0, ReadPosRankSum<-20.0. Effect predictions and annotation was added using snpEFF¹⁰ and dbNSFP¹¹. De-novo variants were detected with GATKs' phase-by-transmission and filtering the Mendelian violations on the de-novo model and coverage >10x for every call.

Sanger sequencing of the coding region and intron-exon boundaries of the *DOCK8* gene was performed on gDNA and cDNA level using specific oligonucleotide primers, as previously described³. Primer sequences are available upon request. Amplified gene fragments were sequenced with an ABI 3730 capillary sequencer (Applied Biosystems, Carlsbad, CA, USA). Mutations were reported using the nomenclature of den Dunnen and Antonarakis.¹²

DOCK8 mRNA expression analyses

Expression levels of DOCK8 splice variants were quantified by an intercalating dye (EvaGreen)-based approach in 96-well plates on a QX200 droplet digital PCR (ddPCR) system with automatic droplet generation (Bio-Rad Laboratories) in duplicates with reaction volumes of 21 μ l, cDNA input of 5-20 ng RNA equivalent, and the following cycling conditions: 5 min at 95 °C, 40 cycles of (30 s at 96 °C, 1 min at 60 °C), 5 min at 4 °C, and 5°min at 90 °C. The following primers (synthesized by Integrated DNA Technologies, IDT) were used at a final concentration of 100 nM: DOCK8.36for: 5-TGC CAC CCT TTA CCT CCT CA-3, DOCK8.37rev: 5-TTC CCA CCA AAG ATG CCA G-3, DOCK8.24for: 5-GCC TGG TTC TTC TTT GAG CTT C-3, DOCK8.26rev: 5-AGA AAG CCA GGC TGA TGT TCA T-3. All ddPCR runs were performed with cDNA of patients or healthy carriers expressing the splice variant (verified by Sanger sequencing), cDNA of healthy individuals as negative control, and purified, nuclease-free water as no-template control (NTC). Droplet fluorescence intensity values were exported from QuantaSoft (Bio-Rad Laboratories). Custom scripts were developed and used to import the intensity values into R (version 3.2.3; <http://www.r-project.org>). To compensate for baseline shifts of fluorescence intensity between reaction wells, data were centered using the following procedure. First, the droplet with the highest fluorescence intensity value in NTC wells was identified and its fluorescence intensity was denoted as maxNTC. Next, droplets in each well were divided into two groups with either low ($\leq 2*\text{maxNTC}$) or high ($> 2*\text{maxNTC}$) intensity. For each well, the median intensity value of the low intensity group of droplets (medianLow) was calculated. Then, for each well, droplet intensity values were normalized by subtracting medianLow from each intensity value. Droplet intensity values were plotted after each step and inspected for negative and positive clusters. In order to automatically assign droplets to one of three groups (negative, positive for splice variant 1, or positive for splice variant 2), k-means clustering with pre-specified number of clusters k was performed for each well.

Target mRNA concentrations c were then calculated for each well from the number of positive droplets Np and negative droplets Nn and the average droplet volume $V = 0.85$ nanoliter based on Poisson distribution statistics using the formula $c = (\ln(Np + Nn) - \ln(Nn))/V$, where \ln is the natural logarithm. For each splice variant, only droplets positive for this particular splice variant were considered positive, and all other droplets were considered negative.

DOCK8 protein assessment

To assess DOCK8 protein expression in different lymphocyte subsets flow cytometry was performed adapted from¹³ using the following antibodies: anti-CD3 APC-H7, anti-CD4 BV711, anti-CD8 PE, anti-CD19 PE-Cy7, anti-CD56 APC (all BD), anti-DOCK8 (SantaCruz), isotype control (Biolegend), and FITC rat anti-mouse IgG (Biolegend). DOCK8 western blot analyses were performed on cells lysed with complete Lysis-M EDTA-free solution (Roche Applied Science, Penzberg, Germany). Following SDS-

4

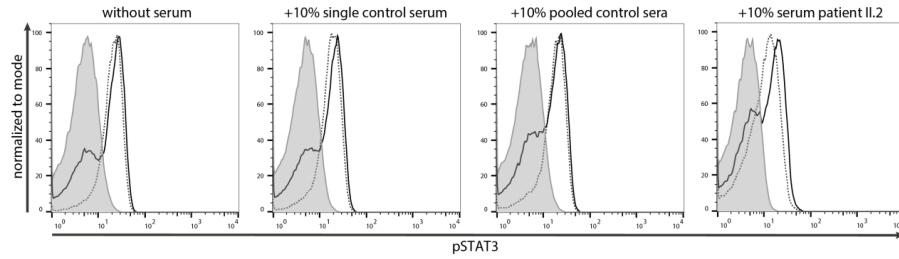
PAGE with NuPAGE Novex 3%-8% Tris-Acetate Gels and transfer with the NuPAGE Large Protein Blotting Kit (Invitrogen, Carlsbad, CA, USA) blots were probed with antibodies to DOCK8 (Abcam, Cambridge, UK and Santa Cruz, Starr County, Texas, USA) and beta-Actin (Cell Signaling, Danvers, MA, USA) and developed with secondary horseradish peroxidase conjugated polyclonal antibodies (Invitrogen, Carlsbad, CA, USA) and SuperSignal West Femto Maximum Sensitivity Substrate (Pierce, Rockford, IL, USA). Spectra Multicolor High Range Protein Ladder (ThermoFisher Scientific, Waltham, MA, USA) was used as size standard.

DOCK8 splicing analyses

Prior to the Sashimi plot and the percent spliced in (psi, Ψ) analysis, the GTEx samples were filtered to obtain a more homogeneous dataset.^{14,15} 2616 samples passed the following filter steps: assembly="HG19_Broad_variant", library_type="cDNAShotgunStrandAgnostic", samples are no technical controls, and molecular_data_type="Allele-Specific Expression". All reads over all samples were pooled together and only reads that mapped around the DOCK8 exons 32 and 36 were included in the Sashimi plots. To evaluate how efficient an intron is spliced out of a transcript, a psi analysis was performed. The Ψ values for the 5' and 3' sites were calculated for each sample as: $\Psi_5(D, A) = \frac{n(D, A)}{\sum_{A'} n(D, A')}$ and $\Psi_3(A, D) = \frac{n(D, A)}{\sum_{D'} n(D', A')}$, where D is a donor site and A is an acceptor site.¹⁶ $n(D, A)$ denotes the number of reads spanning the given junction D-A. The statistic is based on split reads, which are reads spanning multiple exons and having at least one gap in the alignment, the spliced intron. Here the 5' percent spliced in (Ψ_5) value is calculated as the fraction of split reads covering the intron of interest over all split reads covering the given donor site. The 3' percent splice in (Ψ_3) value is calculated the same way but taking the reads covering the acceptor site.

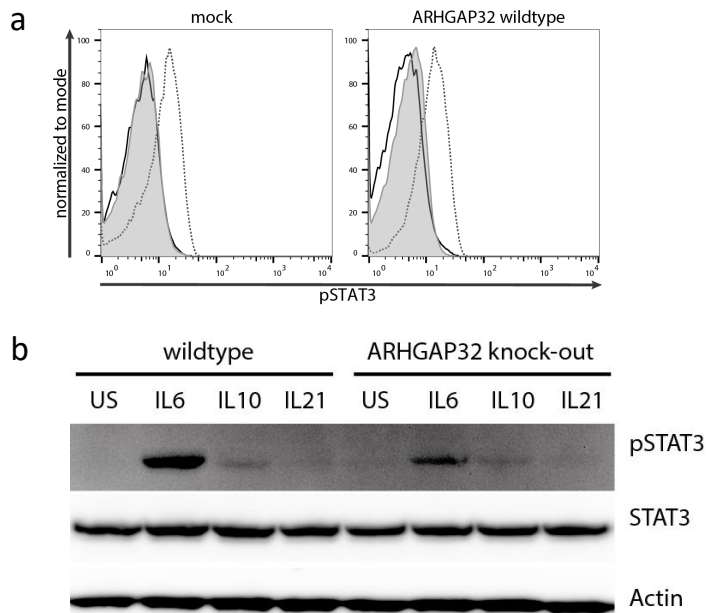
In silico analysis of splice site prediction was performed by utilizing multiple methods: NNSPLICE0.9, Human Splicing Finder (HSF) Version 3.1, SpliceAid2, SplicePort, and CryptSplice.¹⁷⁻²¹ CryptSplice did not obtain results since the variant was too far away from the canonical splice site. Splicing was evaluated by minigene assay. In brief: PBMCs of healthy controls were transiently transfected with a wildtype and a mutated minigene plasmid using the human T-cell nucleofector kit (Lonza, Cologne, Germany) according to manufacturer's instructions. Minigene constructs were generated by cloning a PCR amplicon of human genomic DNA into a pCMV56 vector as previously described.^{22,23} The introduced PCR amplicon started at the first nucleotide of exon 36 to position 25 downstream of exon 37 of *DOCK8* and was flanked by sequence tags to differentiate minigene transcripts from endogenous *DOCK8* transcripts. Transcripts were reverse transcribed using the ProtoScript II First Strand cDNA Synthesis Kit and cDNA was amplified by PCR using the LongAmpTaq 2x Master Mix (both New England Biolabs, Ipswich, MA, USA) according to manufacturer's instruction. The following cycling conditions were used: 3 min at 94 °C, 25 cycles of (30 s at 94 °C, 30 s at 60 °C, 25 s at 65 °C), 10 min at 65 °C, and hold at 4 °C.

Supplementary Figures:



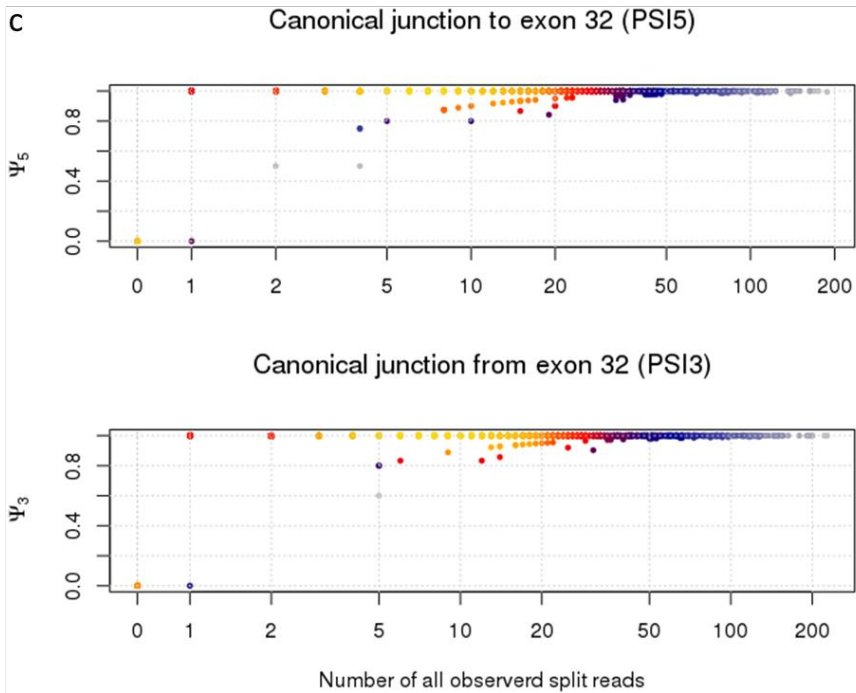
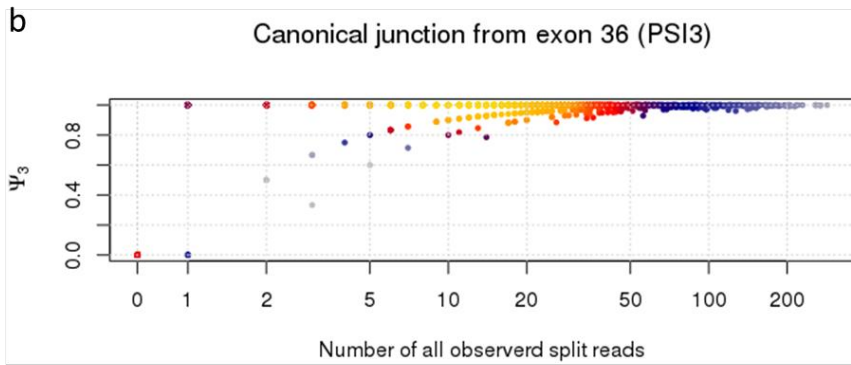
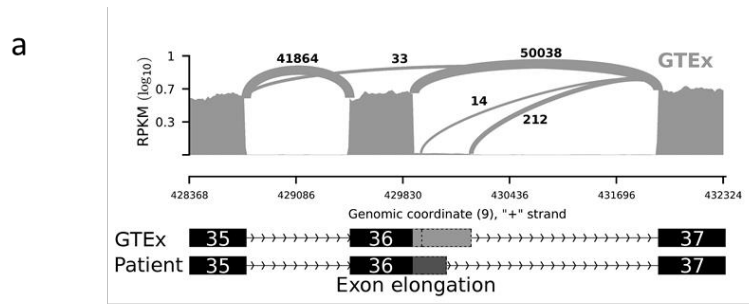
Supplementary Figure S1: Autoantibody analysis.

Flow cytometric analysis showing comparable Y705-STAT3 phosphorylation of lymphocytes after 20 min. stimulation with 200 ng/ml IL6 (solid line) or IL10 (dotted line), incubated with 10% patient or control sera overnight; pooled control sera: sera of seven different healthy controls; filled gray area: unstimulated lymphocytes.



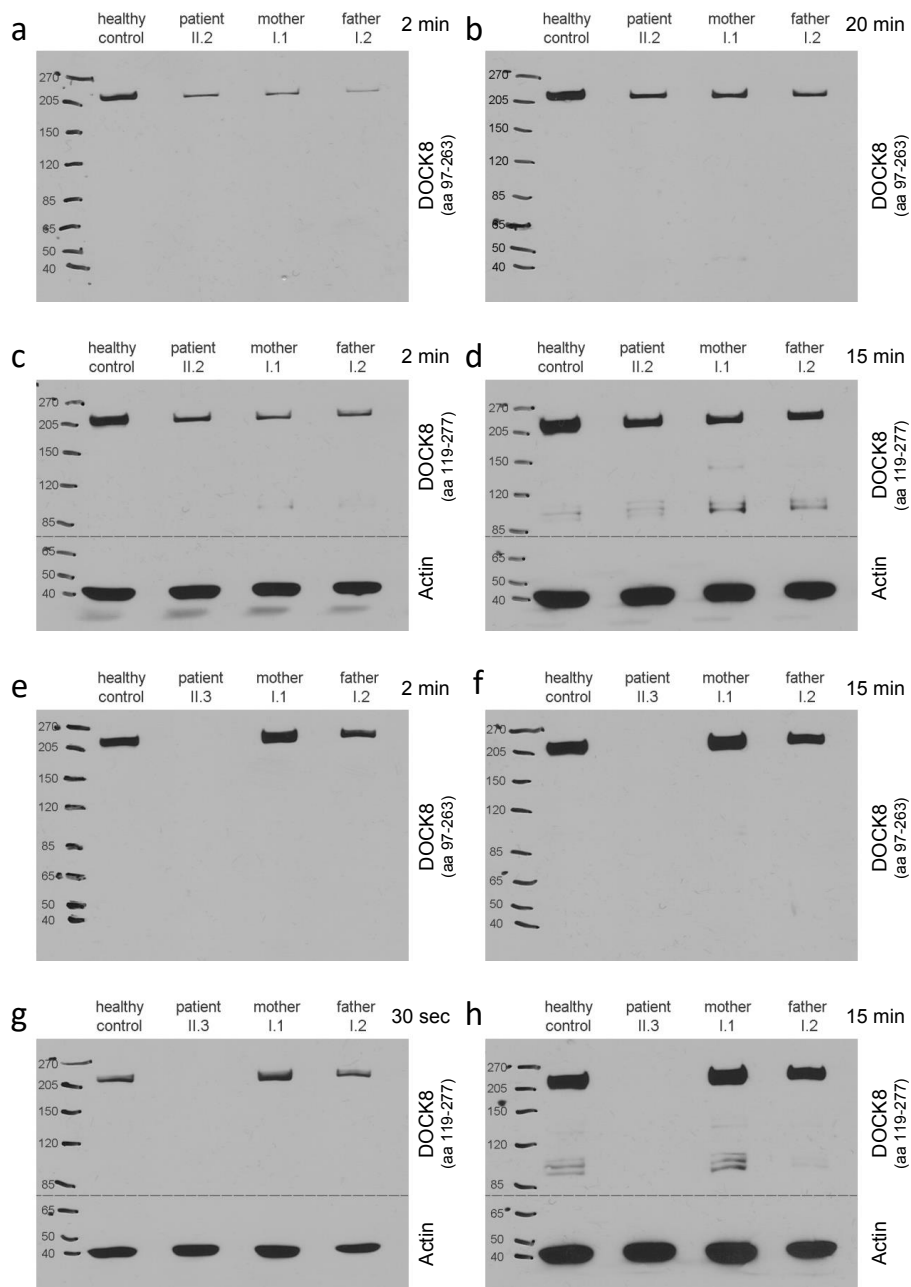
Supplementary Figure S2: ARHGAP32 analysis.

(a) Flow cytometric analysis of Y705-STAT3 phosphorylation of mock- and ARHGAP32-transfected PBMCs of patient II.2 with no rescue of IL6-induced (solid line) Y705-STAT3 phosphorylation by ARHGAP32 overexpression; filled gray area: unstimulated lymphocytes; dotted line: lymphocytes stimulated with IL10. PBMCs were stimulated 20 min. with 200 ng/ml IL6 or IL10. (b) Western blot analysis of whole cell lysates of wildtype and ARHGAP32 knock-out cells, unstimulated or 20 min. stimulated with 20 ng/ml IL6 or IL10, or 10 ng/ml IL21. Expression of STAT3 phosphorylated at Y705 (pSTAT3) and total STAT3 (STAT3) was assessed showing intact stimulation of STAT3 phosphorylation by IL6 in wildtype and ARHGAP32 knock-out cells and no distinct induction of STAT3 phosphorylation by IL10 or IL21 in both cell lines; Actin as loading control.



Supplementary Figure S3: *In silico* analysis of preexisting RNA sequencing data.

(a) Sashimi plot of RNA sequencing data based on GTEx samples^{14,15} showing rare events of exon extension by 16 and 133 nucleotides; read counts accumulated over all samples. (b)(c) Heatscatter plots of Ψ_5 and Ψ_3 values and the total split read counts for all GTEx samples. On the x-axis the overall expression of *DOCK8* at the investigated site (number of all observed reads covering the splice site) is shown against the fraction of transcripts with a spliced intron of interest (Ψ_5/Ψ_3) on the y-axis. Each dot represents one sample. A Ψ value above 0.5 indicates that the intron of interest is spliced out in the majority of the transcripts, while a Ψ value below 0.5 indicates that other isoforms are more favored overall. (b) A heatscatter plot of Ψ_5 values for the donor site of the canonical exon junction between exon 36 and 37 is shown. (c) Heatscatter plots depicting the Ψ_5 and Ψ_3 values of the canonical exon junction between exon 31 and 32 and exon 32 and 33, respectively.



10

Supplementary Figure S4: DOCK8 western blot analysis.

Full-length western blots of whole PBMC lysates of patient II.2 (a-d) and patient II.3 (e-h) in comparison to a healthy control and the parents are shown. Western blots were probed with different DOCK8 antibodies (immunogen indicated in brackets; aa: amino acid) and Actin as a loading control. Western blots were cut at the dashed lines where indicated (c, d, g, h). Exposure times are indicated; sec: seconds, min: minutes.

References:

1. Hagl B, Heinz V, Schlesinger A, et al. Key findings to expedite the diagnosis of hyper-IgE syndromes in infants and young children. *Pediatr Allergy Immunol* 2016;27:177-84.
2. Randall KL, Chan SS, Ma CS, et al. DOCK8 deficiency impairs CD8 T cell survival and function in humans and mice. *J Exp Med* 2011;208:2305-20.
3. Renner ED, Rylaarsdam S, Anover-Sombke S, et al. Novel signal transducer and activator of transcription 3 (STAT3) mutations, reduced T(H)17 cell numbers, and variably defective STAT3 phosphorylation in hyper-IgE syndrome. *J Allergy Clin Immunol* 2008;122:181-7.
4. Puel A, Picard C, Lorrot M, et al. Recurrent staphylococcal cellulitis and subcutaneous abscesses in a child with autoantibodies against IL-6. *J Immunol* 2008;180:647-54.
5. Nijman IJ, van Montfrans JM, Hoogstraat M, et al. Targeted next-generation sequencing: a novel diagnostic tool for primary immunodeficiencies. *J Allergy Clin Immunol* 2014;133:529-34.
6. McKenna A, Hanna M, Banks E, et al. The Genome Analysis Toolkit: a MapReduce framework for analyzing next-generation DNA sequencing data. *Genome Res* 2010;20:1297-303.
7. Van der Auwera GA, Carneiro MO, Hartl C, et al. From FastQ data to high confidence variant calls: the Genome Analysis Toolkit best practices pipeline. *Curr Protoc Bioinformatics* 2013;43:11 0 1-33.
8. van der Auwera GA. Best Practices for Variant Discovery in DNaseq. Broad Institute Genome Analysis Toolkit 2013;<http://gatkforums.broadinstitute.org/gatk/discussion/3238/best-practices-for-variant-discovery-in-dnaseq>.
9. Li H, Durbin R. Fast and accurate short read alignment with Burrows-Wheeler transform. *Bioinformatics* 2009;25:1754-60.
10. Cingolani P, Platts A, Wang le L, et al. A program for annotating and predicting the effects of single nucleotide polymorphisms, SnpEff: SNPs in the genome of *Drosophila melanogaster* strain w1118; iso-2; iso-3. *Fly (Austin)* 2012;6:80-92.
11. Liu X, Jian X, Boerwinkle E. dbNSFP: a lightweight database of human nonsynonymous SNPs and their functional predictions. *Hum Mutat* 2011;32:894-9.
12. den Dunnen JT, Antonarakis SE. Nomenclature for the description of human sequence variations. *Hum Genet* 2001;109:121-4.
13. Pai SY, de Boer H, Massaad MJ, et al. Flow cytometry diagnosis of dedicator of cytokinesis 8 (DOCK8) deficiency. *J Allergy Clin Immunol* 2014;134:221-3.
14. Consortium GT. The Genotype-Tissue Expression (GTEx) project. *Nat Genet* 2013;45:580-5.
15. Consortium GT. Human genomics. The Genotype-Tissue Expression (GTEx) pilot analysis: multitissue gene regulation in humans. *Science* 2015;348:648-60.
16. Pervouchine DD, Knowles DG, Guigo R. Intron-centric estimation of alternative splicing from RNA-seq data. *Bioinformatics* 2013;29:273-4.
17. Reese MG, Eeckman FH, Kulp D, Haussler D. Improved splice site detection in Genie. *J Comput Biol* 1997;4:311-23.
18. Desmet FO, Hamroun D, Lalande M, Collod-Beroud G, Claustres M, Beroud C. Human Splicing Finder: an online bioinformatics tool to predict splicing signals. *Nucleic Acids Res* 2009;37:e67.
19. Dogan RI, Getoor L, Wilbur WJ, Mount SM. SplicePort--an interactive splice-site analysis tool. *Nucleic Acids Res* 2007;35:W285-91.
20. Piva F, Giulietti M, Burini AB, Principato G. SpliceAid 2: a database of human splicing factors expression data and RNA target motifs. *Hum Mutat* 2012;33:81-5.
21. Lee M, Roos P, Sharma N, et al. Systematic Computational Identification of Variants That Activate Exonic and Intronic Cryptic Splice Sites. *Am J Hum Genet* 2017;100:751-65.
22. Forch P, Puig O, Kedersha N, et al. The apoptosis-promoting factor TIA-1 is a regulator of alternative pre-mRNA splicing. *Mol Cell* 2000;6:1089-98.
23. Sakamoto H, Inoue K, Higuchi I, Ono Y, Shimura Y. Control of *Drosophila* Sex-lethal pre-mRNA splicing by its own female-specific product. *Nucleic Acids Res* 1992;20:5533-40.

7 Literaturverzeichnis

1. Notarangelo LD. Primary immunodeficiencies. *J Allergy Clin Immunol.* 2010;125(2 Suppl 2):S182-94.
2. Bousfiha AA, Jeddane L, Ailal F, Al Herz W, Conley ME, Cunningham-Rundles C, et al. A phenotypic approach for IUIS PID classification and diagnosis: guidelines for clinicians at the bedside. *J Clin Immunol.* 2013;33(6):1078-87.
3. Picard C, Al-Herz W, Bousfiha A, Casanova JL, Chatila T, Conley ME, et al. Primary Immunodeficiency Diseases: an Update on the Classification from the International Union of Immunological Societies Expert Committee for Primary Immunodeficiency 2015. *J Clin Immunol.* 2015;35(8):696-726.
4. Picard C, Bobby Gaspar H, Al-Herz W, Bousfiha A, Casanova JL, Chatila T, et al. International Union of Immunological Societies: 2017 Primary Immunodeficiency Diseases Committee Report on Inborn Errors of Immunity. *J Clin Immunol.* 2018;38(1):96-128.
5. Bousfiha A, Jeddane L, Picard C, Ailal F, Bobby Gaspar H, Al-Herz W, et al. The 2017 IUIS Phenotypic Classification for Primary Immunodeficiencies. *J Clin Immunol.* 2018;38(1):129-43.
6. Meyts I, Bosch B, Bolze A, Boisson B, Itan Y, Belkadi A, et al. Exome and genome sequencing for inborn errors of immunity. *J Allergy Clin Immunol.* 2016;138(4):957-69.
7. Holland SM, DeLeo FR, Elloumi HZ, Hsu AP, Uzel G, Brodsky N, et al. STAT3 mutations in the hyper-IgE syndrome. *N Engl J Med.* 2007;357(16):1608-19.
8. Minegishi Y, Saito M, Tsuchiya S, Tsuge I, Takada H, Hara T, et al. Dominant-negative mutations in the DNA-binding domain of STAT3 cause hyper-IgE syndrome. *Nature.* 2007;448(7157):1058-62.
9. Renner ED, Rylaarsdam S, Anover-Sombke S, Rack AL, Reichenbach J, Carey JC, et al. Novel signal transducer and activator of transcription 3 (STAT3) mutations, reduced T(H)17 cell numbers, and variably defective STAT3 phosphorylation in hyper-IgE syndrome. *J Allergy Clin Immunol.* 2008;122(1):181-7.
10. Aydin SE, Kilic SS, Aytakin C, Kumar A, Porras O, Kainulainen L, et al. DOCK8 deficiency: clinical and immunological phenotype and treatment options - a review of 136 patients. *J Clin Immunol.* 2015;35(2):189-98.
11. Su HC. Dedicator of cytokinesis 8 (DOCK8) deficiency. *Curr Opin Allergy Clin Immunol.* 2010;10(6):515-20.
12. Zhang Q, Davis JC, Lamborn IT, Freeman AF, Jing H, Favreau AJ, et al. Combined immunodeficiency associated with DOCK8 mutations. *N Engl J Med.* 2009;361(21):2046-55.
13. Davis SD, Schaller J, Wedgwood RJ. Job's Syndrome. Recurrent, "cold", staphylococcal abscesses. *Lancet.* 1966;1(7445):1013-5.
14. Buckley RH, Wray BB, Belmaker EZ. Extreme hyperimmunoglobulinemia E and undue susceptibility to infection. *Pediatrics.* 1972;49(1):59-70.
15. Grimbacher B, Holland SM, Gallin JI, Greenberg F, Hill SC, Malech HL, et al. Hyper-IgE syndrome with recurrent infections--an autosomal dominant multisystem disorder. *N Engl J Med.* 1999;340(9):692-702.
16. Kroner C, Neumann J, Ley-Zaporozhan J, Hagl B, Meixner I, Spielberger BD, et al. Lung disease in STAT3 hyper-IgE syndrome requires intense therapy. *Allergy.* 2019.

17. Freeman AF, Renner ED, Henderson C, Langenbeck A, Olivier KN, Hsu AP, et al. Lung parenchyma surgery in autosomal dominant hyper-IgE syndrome. *J Clin Immunol*. 2013;33(5):896-902.
18. Grimbacher B, Schaffer AA, Holland SM, Davis J, Gallin JI, Malech HL, et al. Genetic linkage of hyper-IgE syndrome to chromosome 4. *Am J Hum Genet*. 1999;65(3):735-44.
19. Renner ED, Puck JM, Holland SM, Schmitt M, Weiss M, Frosch M, et al. Autosomal recessive hyperimmunoglobulin E syndrome: a distinct disease entity. *J Pediatr*. 2004;144(1):93-9.
20. Boos AC, Hagl B, Schlesinger A, Halm BE, Ballenberger N, Pinarci M, et al. Atopic dermatitis, STAT3- and DOCK8-hyper-IgE syndromes differ in IgE-based sensitization pattern. *Allergy*. 2014;69(7):943-53.
21. Minegishi Y, Saito M, Morio T, Watanabe K, Agematsu K, Tsuchiya S, et al. Human tyrosine kinase 2 deficiency reveals its requisite roles in multiple cytokine signals involved in innate and acquired immunity. *Immunity*. 2006;25(5):745-55.
22. Renner ED, Torgerson TR, Rylaarsdam S, Anover-Sombke S, Golob K, LaFlam T, et al. STAT3 mutation in the original patient with Job's syndrome. *N Engl J Med*. 2007;357(16):1667-8.
23. Schimke LF, Sawalle-Belohradsky J, Roesler J, Wollenberg A, Rack A, Borte M, et al. Diagnostic approach to the hyper-IgE syndromes: immunologic and clinical key findings to differentiate hyper-IgE syndromes from atopic dermatitis. *J Allergy Clin Immunol*. 2010;126(3):611-7 e1.
24. Woellner C, Gertz EM, Schaffer AA, Lagos M, Perro M, Glocker EO, et al. Mutations in STAT3 and diagnostic guidelines for hyper-IgE syndrome. *J Allergy Clin Immunol*. 2010;125(2):424-32 e8.
25. Jiao H, Toth B, Erdos M, Fransson I, Rakoczi E, Balogh I, et al. Novel and recurrent STAT3 mutations in hyper-IgE syndrome patients from different ethnic groups. *Mol Immunol*. 2008;46(1):202-6.
26. Al Khatib S, Keles S, Garcia-Lloret M, Karakoc-Aydiner E, Reisli I, Artac H, et al. Defects along the T(H)17 differentiation pathway underlie genetically distinct forms of the hyper IgE syndrome. *J Allergy Clin Immunol*. 2009;124(2):342-8, 8 e1-5.
27. Engelhardt KR, McGhee S, Winkler S, Sassi A, Woellner C, Lopez-Herrera G, et al. Large deletions and point mutations involving the dedicator of cytokinesis 8 (DOCK8) in the autosomal-recessive form of hyper-IgE syndrome. *J Allergy Clin Immunol*. 2009;124(6):1289-302 e4.
28. Biggs CM, Keles S, Chatila TA. DOCK8 deficiency: Insights into pathophysiology, clinical features and management. *Clin Immunol*. 2017;181:75-82.
29. Aydin SE, Freeman AF, Al-Herz W, Al-Mousa HA, Arnaout RK, Aydin RC, et al. Hematopoietic stem cell transplantation as treatment for patients with DOCK8 deficiency. *J Allergy Clin Immunol Pract*. 2018.
30. Yanagimachi M, Ohya T, Yokosuka T, Kajiwara R, Tanaka F, Goto H, et al. The Potential and Limits of Hematopoietic Stem Cell Transplantation for the Treatment of Autosomal Dominant Hyper-IgE Syndrome. *J Clin Immunol*. 2016;36(5):511-6.
31. Gennery AR, Flood TJ, Abinun M, Cant AJ. Bone marrow transplantation does not correct the hyper IgE syndrome. *Bone Marrow Transplant*. 2000;25(12):1303-5.

8 Danksagung

Besonders bedanken möchte ich mich bei Frau Prof. Dr. med. Ellen Renner für die Überlassung des Themas, die Bereitstellung von wichtigem Patienten- und Labormaterial sowie für ihre stetige Unterstützung in der Formulierung unserer Forschungshypothesen und ihre ausgezeichnete Betreuung. Sie gab mir die Möglichkeit, mein Wissen in den Bereichen der primären Immundefekte und der Allergologie zu erweitern, schaffte es mein Interesse an diesen Fachgebieten immer weiter auszubauen und mich in das wissenschaftliche Arbeiten einzuführen. Nicht zuletzt gab sie mir die Möglichkeit, Ergebnisse meiner Forschungsarbeit zu veröffentlichen und auf Kongressen vorzustellen.

Besonders herzlich bedanken möchte ich mich bei Frau Dr. Beate Hagl, für die sorgsame Einarbeitung in molekularbiologische Techniken und ihre freundschaftliche Unterstützung bei der Umsetzung unserer Forschungsprojekte sowie bei der gesamten Arbeitsgruppe von Frau Prof. Renner für die immer motivierende Zusammenarbeit und herausragende Kollegialität, die die Frustrationsgrenze mehrfach erfolgreich versetzt hat.

Des Weiteren gilt mein Dank den Mitarbeitenden des Immunologischen Diagnostiklabors im Dr. von Haunerschen Kinderspital, Frau Irmgard Eckerlein und Frau Mayumi Hoffman für die stets sehr gute Zusammenarbeit auf begrenztem Raum. Weiterer Dank gilt den Kolleginnen und Kollegen im Forschungskubus des Dr. von Haunerschen Kinderspitals, die uns bei der Umsetzung unserer Forschungsvorhaben unterstützt haben.

Bedanken möchte ich mich ferner bei allen einweisenden Ärzten, den Patienten und deren Familien, durch deren Teilnahme diese Studien erst möglich wurden.

Besonderen Dank möchte ich meiner Freundin Laura sagen, die mich bei der Umsetzung aller Projekte jederzeit unterstützte und besonders bei der Fertigstellung dieser Doktorarbeit stets

motivierend zur Seite stand.

Nicht zuletzt gilt mein außerordentlicher Dank meinen Freunden und meiner Familie, meinen Eltern, und meiner Schwester auf deren Unterstützung ich immer zählen konnte und die mir dieses Studium und die Dissertation erst ermöglichten.

9 Publikationsliste

- 2019 van de Veen W, Krätz CE, McKenzie CI, Aui PM, Neumann J, van Noesel CJM, Wirz OF, Hagl B, Kröner C, **Spielberger BD**, Akdis CA, van Zelm MC, Akdis M, Renner ED. Impaired memory B-cell development and antibody maturation with a skewing toward IgE in patients with STAT3 hyper-IgE syndrome. *Allergy*. 2019 Jul 3. doi: 10.1111/all.13969. **IF 6,0**
- Kröner C, Neumann J, Ley-Zaporozhan J, Hagl B, Meixner I, **Spielberger BD**, Dückers G, Belohradsky BH, Niehues T, Borte M, Rosenecker J, Kappler M, Nährig S, Reu S, Griese M, Renner ED. Lung disease in STAT3 hyper-IgE syndrome requires intense therapy. *Allergy*. 2019 Feb 21. doi: 10.1111/all.13753. **IF 6,0**
- 2018 Hagl B*, **Spielberger BD***, Thoene S, Bonnal S, Mertes C, Winter C, Nijman IJ, Verduin S, Eberherr AC, Puel A, Schindler D, Ruland J, Meitinger T, Gagneur J, Orange JS, van Gijn ME, Renner ED. Somatic alterations compromised molecular diagnosis of DOCK8 hyper-IgE syndrome caused by a novel intronic splice site mutation. *Sci Rep*. 2018 Nov 13;8(1):16719. doi: 10.1038/s41598-018-34953-z. **IF 4,6**
- 2016 Hagl B, Heinz V, Schlesinger A, **Spielberger BD**, Sawalle-Belohradsky J, Senn-Rauh M, Magg T, Boos AC, Hönig M, Schwarz K, Dückers G, von Bernuth H, Christoph P, Karitnig-Weiss C, Belohradsky BH, Josef F, Niehues T, Wahn V, Albert MH, Wollenberg A, Jansson AF, Renner ED. Key findings to expedite the diagnosis of hyper-IgE syndromes in infants and young children. *Pediatr Allergy Immunol*. 2015 Nov 23. doi: 10.1111/pai.12512. **IF 3,8**
- 2014 Boos AC*, Hagl B*, Schlesinger A, Halm BE, Ballenberger N, Pinarci N, Heinz V, Kreilinger D, **Spielberger BD**, Schimke-Marquez LF, Sawalle-Belohradsky J, Belohradsky BH, Pryzbilla B, Schaub B, Wollenberg B, Renner ED. Atopic dermatitis, STAT3- and DOCK8-hyper-IgE syndromes differ in IgE-based sensitization pattern. *Allergy* 2014; doi:10.1111/all.12416 **IF 7,3**
- 2012 **Spielberger BD**, Woellner C, Dueckers G, Sawalle-Belohradsky J, Hagl B, Anslinger K, Bayer B, Siepermann K, Niehues T, Grimbacher B, Belohradsky BH, Renner ED. Challenges of genetic counseling in patients with autosomal dominant diseases, such as the hyper-IgE syndrome (STAT3-HIES). *J Allergy Clin Immunol*. 2012 Dec;130(6):1426-8. **IF 13,1**

* contributed equally

